

## **Influence of seep emission on the non-symbiont-bearing fauna and vagrant species at an active giant pockmark in the Gulf of Guinea (Congo–Angola margin)**

K. Olu<sup>a,\*</sup>, J.C. Caprais<sup>a</sup>, J. Galéron<sup>a</sup>, R. Causse<sup>b</sup>, R. von Cosel<sup>c</sup>, H. Budzinski<sup>d</sup>, K. Le Ménach<sup>d</sup>, C. Le Roux<sup>e</sup>, D. Levaché<sup>f</sup>, A. Khripounoff<sup>a</sup> and M. Sibuet<sup>a</sup>

<sup>a</sup> Département Etude des Ecosystèmes Profonds, IFREMER Centre de Brest, BP70-29280, Plouzané, France

<sup>b</sup> Muséum National d'Histoire Naturelle, UMR 5178 BOME-DMPA, 43 Rue Cuvier-75231 Cedex 05 Paris, France

<sup>c</sup> Muséum National d'Histoire Naturelle, USM 602 Taxonomie et Collections, 51-57, Rue Cuvier-75231 Cedex 05 Paris, France

<sup>d</sup> Université Bordeaux, ISM/LPTC, UMR 5255 CNRS, 351 crs de la Libération, 33405 Talence, France

<sup>e</sup> Station Biologique de Roscoff, UMR CNRS-UPMC 7144, Place Georges Teissier, 29682 Roscoff, Cedex, France

<sup>f</sup> TOTAL Exploration Production, CSTJF Avenue Larribau 64018 Pau Cedex, France

\*: Corresponding author : K. Olu, Tel.: 33 2 98 22 46 57; fax: 33 2 98 22 47 57, email address : [Karine.Olu@ifremer.fr](mailto:Karine.Olu@ifremer.fr)

### **Abstract:**

Detailed surveying with an ROV found that a dense and diverse cold-seep community colonises a giant pockmark located at 3200 m depth, 8 km north from the deep Congo channel. Several types of assemblages, either dominated by Mytilidae and Vesicomidae bivalves or Siboglinidae polychaetes, are distributed on the 800-m diameter active area. The site is characterised by a most active central zone in a depression with abundant carbonate concretions and high methane fluxes where high-density clusters of mussels and siboglinids dominate. In contrast, the peripheral zones display large fields of dead and live vesicomids on soft sediment, with a lower mean density and lower methane concentration in seawater. The associated megafauna includes Alvinocarididae shrimps, echinoids, holothurians of the family Synaptidae, several species of gastropods, two species of galatheids, and Zoarcidae and Ophiidiidae fishes. Multivariate analyses of video transect data show that the distribution of these major megafauna species at the pockmark scale is influenced by the habitat heterogeneity due to fluid or gas emission, occurrence of hydrates, substratum variability and by the presence of large symbiont-bearing species. Several assemblages dominated either by mytilids, vesicomids, or siboglinids have been sampled for megafauna densities and biomass estimations and stable isotope measurements ( $\delta^{13}\text{C}$  and  $\delta^{15}\text{N}$ ) of dominant species and food sources. The highest estimates of megafauna densities have been obtained in mytilid beds. According to their stable isotopes values, non-symbiont-bearing species mainly rely on chemosynthesis-originated carbon, either as primary consumers of chemoautotrophic microorganisms, or at higher trophic level recycling organic matter, or relying on bivalve and tubeworm production. Most of them likely feed on different sources like shrimps, but differences according to habitat have been evidenced. Carbon and nitrogen isotope ratios of galatheids and benthic or benthopelagic fishes captured by trawls at increasing distances from the pockmark provide evidence of the high variability in the proportion of chemosynthesis-originated carbon in their diet, from 15% to 38%, according to the species captured as far as 4 km to the site.

**Keywords:** Cold seep; Megafauna; Isotopic signature; Vagrant species; Atlantic Equatorial African margin; Congo–Angola margin

54  
55  
56  
57  
58  
59  
60  
61  
62  
63  
64  
65  
66  
67  
68  
69  
70  
71  
72  
73  
74  
75  
76  
77  
78

## 1. Introduction

In deep chemosynthetic environments driven by fluids enriched in methane and sulphide, i.e. hydrothermal vents and cold seeps, extreme habitat heterogeneity and variability suggest that communities are mainly structured by abiotic forces (e.g., Barry et al., 1997; Bergquist et al., 2005; Henry et al., 1992; Levin et al., 2003; MacDonald et al., 2003; Olu et al., 1997; Sahling et al., 2002; Sarrazin et al., 1999; Van Dover, 1995). Nevertheless, the high biomass which characterizes these environments suggests that biotic interactions should also be important community structuring factors at seeps like at vents (Levesque et al., 2003; Micheli et al., 2002; Sarrazin and Juniper, 1999; Tunnicliffe, 1991).

Megafauna, or large-size epifauna at cold seeps, which are associated with biomass-dominant symbiont-bearing species, include high diversity of taxa and almost all the marine phyla (Levin, 2005; Sibuet and Olu, 1998). Diverse communities are probably favoured by substratum heterogeneity that includes both soft bottoms and carbonate concretions, and as well as environmental conditions that are moderate compared to hydrothermal vents. Symbiont-bearing megafauna are also considered as a source of habitat heterogeneity, because they generate extensive habitat complexity (Levin 2005). Megafaunal community structure and diversity are highly variable among seep sites, and are thought to be influenced by factors such as depth, substratum, pelagic or terrestrial inputs (Levin et al., 2000; Levin and Michener, 2002; Sahling et al., 2003; Sibuet and Olu-Le Roy, 2002; Sibuet and Olu, 1998), patch size or age of symbiont-bearing species (Cordes et al., 2005; MacAvoy et al., 2005).

Dense chemosynthetic communities were discovered on a large part of a 800-m-diameter pockmark discovered along the Congo-Angola margin a few kilometres from the Congo deep

79 channel (Olu-Le Roy et al., 2007a; Ondréas et al., 2005). These first studies described  
80 assemblages visually dominated by symbiont-bearing taxa, Vesicomidae and Mytilidae  
81 bivalves and Siboglinidae polychaetes whose distributions seemed to be controlled by  
82 methane fluxes and substratum variability. This giant pockmark is, in fact, a complex (a  
83 pockmark ‘cluster’) of several individual pockmarks of about 100 m in diameter whose  
84 variable activities may contribute to the spatial heterogeneity observed on the seafloor  
85 (Ondreas et al. 2005). The distribution of other megafaunal species is probably controlled by  
86 habitat heterogeneity occurring at the pockmark scale, which is created both by fluid  
87 emission-related patterns and by the symbiont-bearing species, serving as ‘ecosystem  
88 engineers’ according to Levin (2005).

89 Following Carney (1994), associated fauna may be classified as endemic, colonist, and  
90 vagrant, depending on their abundance at seeps compared to background areas. Stable  
91 isotopes, which were first used to demonstrate chemosynthesis processes in seep community,  
92 and were mainly applied to symbiont-bearing species (Kennicutt II et al., 1992; Paull et al.,  
93 1984; Paull et al., 1985; Rau and Hedges, 1979), can be used to estimate trophic dependence  
94 of these ‘associate’ or ‘heterotrophic’ species on chemosynthetic production (Levin et al.,  
95 2000; Levin and Michener, 2002; MacAvoy et al., 2002). Carbon and nitrogen stable isotopes  
96 also have been used to decipher nutritional associations among fauna at vents (Colaço et al.,  
97 2002; Fisher et al., 1994; Levesque et al., 2006; Polz et al., 1998; Van Dover, 2002; Van  
98 Dover and Fry, 1989; Vereshchaka et al., 2000) and, more recently, at seeps (MacAvoy et al.,  
99 2005; Van Dover et al., 2003). The fauna closely associated with tube worm aggregations at  
100 cold seeps in the Gulf of Mexico obtain the bulk of its nutrition from local sources of primary  
101 production (MacAvoy et al. 2005) but the relative importance of chemosynthetic pathways  
102 have been suggested to vary regionally with depth and among microhabitats defined by  
103 dominant symbiont-bearing species (Levin and Michener, 2002).

104

105 The objective of the present study is to assess the influence of seep emissions on the non-  
106 symbiont-bearing megafauna at a giant pockmark recently discovered, and therefore the  
107 dependence of these species on the seep energy, by analysing the following: (i) species  
108 distribution relative to the distribution of active seeps at the pockmark scale, (ii) densities and  
109 biomass at more or less active local seeps, and (iii) isotopic signature of their tissues relative  
110 to chemoautotrophic or external sources of carbon and nitrogen. Export of local  
111 chemosynthetic biomass by large mobile predators captured in the background of the deep  
112 seep site is also estimated from stable isotope measurements.

113

114

## 115 2. Materials and methods

116

### 117 2.1. Video survey and image analysis for megafauna distribution

118 The giant pockmark named 'REGAB' (Ondréas et al. 2005) was explored by the ROV Victor  
119 6000 in 2001 during the Ifremer-TOTAL collaborative programmes ZAIANGO and  
120 BIOZAIRE (Sibuet and Vangriesheim, 2009). This active cold-seep site is located at 3170 m  
121 depth on the Gabon continental margin close to the deep Congo channel (5°47,50'S;  
122 9°42'40"E) (Figure 1). In this paper we will use the term 'pockmark' for the whole pockmark  
123 area, not to describe individual pockmarks. Regularly spaced video transects were first  
124 performed on the whole structure (Figure 2). Different types of faunal assemblages forming  
125 clusters were subsequently defined and mapped (Olu-le Roy et al. 2007a; Figure 2) within the  
126 pockmark; they were defined as 'chemosynthetic assemblages' and either dominated by  
127 large bushes of the siboglinid polychaete *Escarpia southwardae* Andersen et al. 2005, or by  
128 two species of vesicomid bivalves undistinguishable on images but identified from samples

129 as *Laubiericoncha chuni* (Thiele and Jaeckel, 1931), see Cosel and Olu (2008) and  
130 *Caplytogenia regab* Cosel and Olu (2009), or by the Mytilidae *Bathymodiolus* sp. aff.  
131 *boomerang* (Olu-Le Roy et al., 2007b). The results of a second phase of video analysis,  
132 subsequent to the symbiont-bearing species cluster mapping, are presented in this paper.  
133 Video surveys of seven dives were analysed in order to map the distribution of megafaunal  
134 associate species along the dive tracks, at the pockmark scale. The video sequences from a  
135 down-looking camera, which was vertically mounted on the ROV, during 3-m-altitude  
136 surveys were analysed for the distribution of visible taxa of at least a 2-cm size, including the  
137 largest gastropods, some crustaceans, echinoderms and fishes. Maps of distribution along the  
138 dive tracks were compiled for the dominant associated species and compared with the  
139 previously acquired distribution maps of symbiont-bearing species, using the ADELIE  
140 extension for ArcGIS 9.0 developed at Ifremer. Each taxon record was associated with visual  
141 observations of habitat including the following: (i) substratum category (soft sediment,  
142 carbonate concretions, hydrate outcrops) and (ii) dominant symbiont-bearing species (living  
143 or dead vesicomyids, mytilids, siboglinids) or bacterial mats. Multidimensional scaling  
144 (MDS) of the species/biotope matrix of distance using the Bray Curtis distance (Primer  
145 software) was performed to identify the relationships between megafauna distribution and  
146 habitat characteristics.

147 In order to compare density and biomass of the associated megafauna in the clusters  
148 dominated by different symbiont-bearing species, 11 assemblages or 'sites' were selected at  
149 different locations on the pockmark, either in the central, more active part of the pockmark  
150 for methane emission (Charlou et al., 2004), or in peripheral areas (Table 1). There were  
151 three assemblages of different sizes dominated by *Bathymodiolus* aff. *boomerang*, five  
152 vesicomyid clusters with different proportion of living and dead individuals, and located in  
153 the different zones of the pockmark, and two escarpiid *E. southwardae* one, presumed to be

154 adults and the other one juveniles. Density, biomass of dominant symbiont-bearing species  
155 and also chemical characteristics at each site are described in Olu Le Roy et al. (2007a).  
156 Megafaunal species densities, when making density estimates on surfaces, were either  
157 estimated from close-up views using four laser points spaced 23 cm apart or from the scale  
158 provided by the ROV's sampling tools. When possible, density was averaged from five to 10  
159 sequential, but non-overlapping images or from complete mosaics of the same site, produced  
160 from short video sequences using the ADELIE software. Individual wet weights were  
161 estimated from formalin-preserved specimens collected by the ROV grab or suction sampler,  
162 and dry weights of same specimens after 48 h at 60°C. Species biomass in the assemblages  
163 was estimated from three to five specimens of different sizes for each species.

164

## 165 2.2. Stable isotope measurements

166 Carbon and nitrogen isotopic ratios were analysed for three symbiont-bearing species and ten  
167 associated species, sampled by ROV in the chemoautotrophic assemblages. Between two and  
168 five individuals were analysed for each species. With this sample set, it was possible to  
169 correlate isotopic signature to habitat for associated species collected in multiple assemblages  
170 that were dominated by different symbiont-bearing species. Specimens used for isotopic  
171 measurements were dissected on board; muscle samples were removed and stored in liquid  
172 nitrogen. In the laboratory, samples were dried under vacuum and analysed in triplicate for  
173 their carbon and nitrogen isotopic ratios ( $\delta^{13}\text{C}$  and  $\delta^{15}\text{N}$ ) calculated by a DELTA Plus  
174 (thermo Finnigan) isotopic mass spectrometer (LPTC, Bordeaux) and for a few samples by a  
175 FINNIGAN DELTA S IRMS (Station Biologique de Roscoff) as follows:

176

$$\delta^x \text{E} = \left[ \frac{\left( \frac{{}^x\text{E}}{{}^y\text{E}} \right)_{\text{sample}}}{\left( \frac{{}^x\text{E}}{{}^y\text{E}} \right)_{\text{standard}}} - 1 \right] \times 1000$$

177 where  $E$  is the element analysed (C or N),  $x$  is the atomic weight of the heavier isotope, and  $y$   
178 is the atomic weight of the lighter isotope ( $x = 13, 15$  and  $y = 12, 14$  for C and N,  
179 respectively). The standard materials to which the samples were compared were PDB (Pee  
180 Dee Belemnite) for carbon and air N<sub>2</sub> for nitrogen. Reproducibility of all measurements was  
181 about 0.3‰. The standard compounds used to correct samples' values from deviation due to  
182 the spectrometer were usg24 (16.1‰) for the carbon and N1 (0.4‰) for the nitrogen. Inter-  
183 comparison of measurements was performed to test the reproducibility of the samples  
184 analysed by the two mass spectrometers.

185 In addition to the fauna, sediments from ROV push cores collected adjacent to the different  
186 assemblages were analysed after vertical subsampling of 2-cm slices from the interface (0  
187 cm) to a depth of 6 cm. Isotopic measurements were performed after acidification to remove  
188 carbonates. Particles from sediment traps deployed for a year on the REGAB site, at 400 m  
189 above the seafloor, were also analysed for carbon and nitrogen isotopic ratios.

190 Methane  $\delta^{13}\text{C}$  was measured on sediment from tube-cores (first 5 cm) collected in crimping  
191 boxes and on water in sealed vials (20 ml) and analysed by Head-Space/Gas  
192 Chromatography/Isotope Ratio Mass Spectrometry (HS/GC/IRMS) in Total Laboratory.

193

194 The REGAB and background megafauna were also sampled by beam trawls. Trawl samples  
195 were taken at increasing distances from the centre of the pockmark as follow: at 400  
196 (peripheral edge), 580, 1560, 3680 and 5800 m, southward (CP19 to CP15), and at 610, 680,  
197 1660 and 3600 m northward (CP20 to CP23) (Figure 1b). Benthic fishes and galatheids were  
198 analysed for their isotopic composition, with particular attention being paid to species  
199 collected in the cold-seep site and in the background. Pieces of tail muscles of 38 specimens  
200 belonging to 12 species of fishes and abdomen muscles of 9 specimens of galatheids were  
201 dissected on board. The proportion of chemosynthetic carbon in the diet of these mobile

202 predators or scavengers was estimated with the following isotopic mixing equation proposed  
203 by MacAvoy et al. (2002):

$$204 \delta x E_{predator} - F = (\delta x E_{seep} \times f_{seep}) + (\delta x E_{ocean} \times (1 - f_{seep})) \quad (1)$$

205 where  $f_{seep}$  is the fraction of diet from chemosynthetic sources and  $\delta x E_{seep}$  and  $\delta x E_{ocean}$   
206 are the mean isotopic signatures of the chemosynthetic material and background ocean,  
207 respectively. The parameter  $F$  corrects for trophic enrichment and is dependent on the isotope  
208 used. When using  $\delta^{13}\text{C}$  and  $\delta^{15}\text{N}$ ,  $F$  was given a value of 1 and 3.5‰, respectively, which is  
209 the trophic enrichment typically associated with these isotopes (Minegawa and Wada, 1984;  
210 Rau et al., 1983) The values used for the mean isotopic signatures of the chemosynthetic  
211 prey,  $\delta x E_{seep}$  ( $\delta^{13}\text{C}_{seep}$  and  $\delta^{15}\text{N}_{seep}$ ), were calculated by averaging values for selected  
212 resident fauna exclusive of vagrant species, and for sediment collected at different places in  
213 the active site. The phytodetritus-based food sources of the background,  $\delta x E_{ocean}$ , were  
214 similarly estimated from values of megafauna species collected in the same beam trawl  
215 samples as fishes, except for the one sampling part of the cold-seep site (CP20). This trawl  
216 haul (CP20) was performed in the north part of the pockmark and collected some species of  
217 the chemoautotrophic assemblages characteristics of the cold-seep site. Some of these species  
218 were analysed for their isotopic signature, in order to increase the number of specimens, but  
219 were separated in the results, as they cannot be referred to a particular habitat (e.g., mussel  
220 bed, etc.) as for ROV samples.

221

### 222 3. Results

#### 223 3.1. Distribution of megafauna species all over the pockmark

224 On the giant pockmark, 10 invertebrate taxa were identified on videos as associate species of  
225 chemosynthetic assemblages; their occurrence is reported together with substratum and  
226 symbiont-bearing species, to characterise the habitat. A total of 4352 individuals were

227 counted along video tracks, with half being galatheids ascribed to *Munidopsis* sp.. The  
228 species were not recognizable on the images, but *Munidopsis geyeri* was more abundant in  
229 the samples than was *Munidopsis hirtella* (Macpherson and Segonzac, 2005). Shrimps  
230 described from samples as *Alvinocaris muricola* (Komai and Segonzac, 2005), holothurians  
231 of the genus *Chiridota*, a species close to *Chiridota heveva* Pawson and Vance, 2004 (M.  
232 Sibuet, pers. com.) and large gastropods of family Turridae, species *Phymorhynchus coseli*  
233 Warén and Bouchet (2009) were also well represented. Other taxa are irregular echinoids and  
234 several families of fishes, including the families Zoarcidae, Macrouridae and Ophidiidae,  
235 which were the most abundant and easily recognisable. The distribution maps (Figure 3) of  
236 the four most abundant taxa (*Munidopsis* sp., *Alvinocaris muricola*, *Chiridota* sp. and  
237 echinids) show that, galatheids were observed along the dive tracks throughout the pockmark,  
238 while the other species seem to be closely associated with fluid emission, as co-occur with  
239 symbiont-bearing species. Shrimps were mainly observed in the central part of the pockmark  
240 associated with mytilid and escarpiid assemblages; echinids were only observed in soft  
241 sediment areas, in the close vicinity of vesicomid beds, and holothurians were observed in  
242 the entire active area. Multivariate analyses were performed for the entire data set to avoid  
243 misinterpretation due to denser sampling coverage in the active region. The result of the  
244 multidimensional scaling analysis, using the Bray Curtis distance between species and  
245 analysing first the similarity between biotopes (Figure 4a), identified the symbiont-bearing  
246 species assemblages (mytilids, vesicomids and escarpiids), as the exception of dead  
247 escarpiid bushes, as a primary habitat for associated megafauna, the bare substratum (soft,  
248 reduced sediment, carbonate) as a secondary habitat and hydrate outcrops, dense gas bubbles  
249 and bacterial mats as a final one (stress = 0.03). Analysis of the similarity between species  
250 (Figure 4b) grouped together Alvinocarid shrimps, *Chiridota* sp. holothurians, species  
251 associated with living symbiont-bearing species assemblages and, to a lesser degree,

252 galatheids (stress = 0.02). Whether or not *Phymorrhynchus* belongs to this group depends on  
253 the ‘classification’ or grouping method employed. Its relationship with symbiont-bearing  
254 species is much less strong than for other species. The zoarcid fish *Lycodes* sp. and echinoids  
255 are grouped together; they were generally both observed in the close vicinity of symbiont-  
256 bearing bivalve assemblages. Other fishes and swimming holothurians defined another group,  
257 whose distribution is probably independent of that of chemosynthetic fauna.

258

### 259 3.2. Megafaunal community structure in chemosynthetic assemblages

260

261 The densities of megafaunal species were estimated from images at 10 sites, which were  
262 either characterised as vesicomys, mytilid clusters, or escarpiid bushes (Tables 2a and 2b).  
263 The symbiont-bearing species generally show the highest densities in clusters with 31 to 86%  
264 of the total individuals, and largely dominate the megafaunal biomass with 71-76% in  
265 escarpiid bushes and 84-98% in bivalve clusters. The associated species observed in the  
266 symbiont-bearing species clusters are dominated by the shrimps *Alvinocaris muricola*,  
267 independent of the symbiont-bearing species, except in the vesicomys clusters V1 and Vext.  
268 Their very high density, up to 744 ind.m<sup>-2</sup> in mytilid beds, 246 ind.m<sup>-2</sup> in vesicomys clusters  
269 and 302 ind.m<sup>-2</sup> in escarpiid bushes, represents between up to 12% of the total biomass in dry  
270 weight in bivalve clusters and up to 26% in escarpiid bushes. The gastropods include the  
271 Provannidae *Provanna reticulata* Warén and Bouchet (2009) and *Provanna chevalieri* Warén  
272 and Bouchet (2009) (not distinguishable on images) and the limpet *Paralepetopsis sasakii*  
273 Warén and Bouchet (2009). Both genera have high numerical densities in mytilid beds and  
274 adult tube-worm bushes. Nevertheless, owing to their small size, they make a small  
275 contribution to the total biomass. In the vesicomys clusters, their densities are more variable,

276 only the Provannidae are present, in association with high bivalve density (>500 ind./m<sup>2</sup>).  
277 The Turridae *Phymorrhynchus coseli* is sometimes associated with vesicomysids in soft  
278 sediment areas in the SW part of the pockmark in clusters with numerous empty shells  
279 (V1,VB). Actiniaria colonise concretions and among mussels. The holothurid *Chiridota* sp.  
280 can be locally abundant, particularly among bivalves, and has higher densities in vesicomysid  
281 clusters than in mytilid beds. *Munidopsis geyeri* is only observed in the clusters located in the  
282 periphery areas. The zoarcid fish *Lycodes* sp. is commonly observed among bivalves, but not  
283 with high densities (no more than one or two ind/cluster).

284 The densities and biomass of associated species were highest in the three mytilid beds (Table  
285 2), whereas among vesicomysid clusters and escarpiid bushes they have lower  
286 densities/biomass. These differences are only significant for density and biomass between  
287 mytilid and vesicomysids assemblages (Kruskall Wallis test; p value<0.05). The densities and  
288 biomass are highly variable in vesicomysid clusters, and higher in the adult escarpiid bush  
289 than in the juvenile one. Among the vesicomysids, densities of associated species mainly  
290 depend on the bivalve density, but also on their location in the pockmark. The clusters  
291 located in the central part of the REGAB site (V3 and VC) have higher densities, particularly  
292 of *Alvinocharis muricola* and *Provanna* sp. than V1 and VB that are located in the peripheral  
293 fields and Vext, which is an isolated cluster away from the active part of the pockmark  
294 (Figure 2b). Considering the total density of the symbiont-bearing and non-symbiont-bearing  
295 species, the density and biomass of mytilid clusters are significantly higher than in the other  
296 two cluster types (mean = 1882 ind.m<sup>-2</sup>, 691 ind.m<sup>-2</sup> and 629 ind.m<sup>-2</sup>, respectively, for  
297 vesicomysids and escarpiid assemblages).

298

299

300 *3.3. Isotopic measurements*

301 3.3.1. Sources: methane, particles from traps and sediment

302 Methane carbon isotopic ratio measured from sediment samples varies from  $-68.5$  to  $-96.2$   
303 ‰ (mean =  $-80.23$  ‰, sd = 9.58, n=7) (Table 3). The values were more homogeneous in the  
304 four water samples analysed with a mean  $\delta^{13}\text{C}$  of  $-68.57$ ‰ (sd = 1.34). Methane was the  
305 main component of the hydrocarbon gas extracted from sediment (98.8 %) and water (99.97  
306 %).

307 The organic matter obtained in particle traps partly contained detrital matter from a  
308 terrestrial origin (Treignier et al. 2006). Its  $\delta^{13}\text{C}$  value ( $-23.22$ ‰) is consistent with this  
309 origin and with the  $\delta^{13}\text{C}$  value of sediments sampled off the cold-seep site (Table 4) while the  
310  $\delta^{15}\text{N}$  (4.43‰) is lower due to less recycling. The  $\delta^{13}\text{C}$  of the sediment sampled next to the  
311 different types of assemblages in the active site is depleted compared with these values and  
312 on average is more depleted close to mytilid than vesicomid clusters (Table 4). The  
313 microorganism community, which probably contributes significantly to the carbon pool in the  
314 sediment, may have a different composition depending on the site and environment  
315 (Cambon-Bonavita et al., 2009) and thus a different signature.  $\delta^{15}\text{N}$  values show a strong  
316 contrast between mytilid and vesicomid surrounding sediments. The values close to zero are  
317 probably due to a higher contribution of the microbial primary producers compartment to the  
318 sediment close to the mytilids, where the methane fluxes are higher than close to vesicomids  
319 (Olu-Le Roy et al. 2007a), while the less depleted  $\delta^{15}\text{N}$  values close to less active areas  
320 colonised by vesicomids may indicate a higher content of detrital/recycled material.

321

322

323 3.3.2. Chemoautotrophic symbiont-containing species

324 *Bathymodiolus* aff. *boomerang* tissues have quite homogeneous isotopic signatures and  
325 demonstrated the most depleted values (Table 5), consistent with dominant nutrition via

326 methanotrophic symbionts. Mussels from the M2 site are significantly more depleted in  $\delta^{13}\text{C}$ ,  
327 particularly the gills ( $-67.05\text{‰}$ ), than those from M1 and M3. Only at M2, have gills  
328 significantly different  $\delta^{13}\text{C}$  than from the mantle.

329 The relative importance of methanotrophy vs. sulphide oxidation in the nutrition of the  
330 mussels can be estimated by a two-end-member mixing equation (Fry and Sherr, 1984)  
331 where:

332  $\delta^{13}\text{C}_{consumer} = f \times \delta^{13}\text{C}_{source 1} + (1-f) \times \delta^{13}\text{C}_{source 2}$  (2) where  $f$  is the proportion of  
333 carbon originated from *source 1* in the nutrition of the consumer.

334 or by Equation (1) :  $\delta x E_{predator} - F = (\delta x E_{seep} \times f) + (\delta x E_{ocean} \times (1-f))$  (1) already cited,  
335 taking into account the parameter  $F$  that corrects for trophic enrichment. We used  $F = 1$   
336 between carbon source and mussels, as isotopic fractionation is negligible during  
337 methanotrophy, from carbon source to the symbionts (Conway et al., 1994), and the two  
338 possible carbon sources are the  $\text{CH}_4$ -derived carbon ( $\delta^{13}\text{C} = 67-70 \text{‰}$ ) and DIC ( $\delta^{13}\text{C} = 23$   
339  $\text{‰}$ ). The estimated contribution of methanotrophy in the mussel nutrition is, following the  
340 Fry and Sherr equation (2), from 84 to 100% and following MacAvoy equation (1) from 85 to  
341 88%. Equation (2) was used by Van Dover et al. (2003) to estimate the relative importance of  
342 methanotrophy (source 1) vs. sulphide oxidation (source 2) in the nutrition of mussels,  
343 assuming that photosynthetically derived material is negligible. Considering the methane  
344 signature as carbon source (1) and the vesicomid signature for thiotrophically generated  
345 biomass as source (2), REGAB mytilids has a contribution of methanotrophy from 76 to  
346 94%. Vesicomids showed typical values for sulphur-oxidizing symbionts, with no  
347 significant differences between sites (V1/V3) or tissues. Escarpiids were characterised by  
348 more heterogeneous signatures, with significantly different values between sites with the less  
349 depleted at M1, dominated by mytilids, and the more for the adult bush EA. Juveniles

350 sampled at EB had an intermediate isotopic signature, between those of adults from EA and  
351 M1.

352

### 353 3.3.3. Associate megafauna in chemosynthetic assemblages

354 Results of the 55 individuals of 10 species of presumably non-symbiont-bearing invertebrates  
355 analysed for carbon and nitrogen stable isotopes are summarised in Table 6 and plotted in  
356 Figure 5. The tissue  $\delta^{13}\text{C}$  values of the species collected either during ROV dives in  
357 chemoautotrophic assemblages or by the trawl haul realised in the north part of the pockmark  
358 (CP20) ranged from  $-35.12$  to  $-60.09\text{‰}$  and revealed that the major part of their diet is from  
359 a chemoautotrophic origin. Indeed, POM from particle traps has  $\delta^{13}\text{C}$  value of  $-23.22\text{‰}$   
360 (Table 4). The sole exception is the galatheid *Munidopsis hirtella* ( $\delta^{13}\text{C} = -22.4\text{‰}$ ) only  
361 collected in the trawl, that is probably an occasional or vagrant species in the cold-seep site.  
362 The  $\delta^{15}\text{N}$  values, ranging from 1.9 to 9.37‰, suggest that the majority of individuals derive  
363 their nutrition heterotrophically rather than from symbionts.

364 The isotopic signature of individuals collected by trawls in the north part of the pockmark (*A.*  
365 *muricola* and *Chiridota* sp.) compared with those sampled by ROV in the central part of the  
366 pockmark showed a lesser contribution of chemosynthesis-based production in their diet  
367 ( $-20\text{‰}$  shift in  $\delta^{13}\text{C}$  for the holothurid). The commensal polychaete *Branchipolynoe* sp.  
368 collected in *Bathymodiolus* mussels has a  $\delta^{13}\text{C}$  signature very close to its host. The grazers  
369 including the gastropods *Provanna* and *Paralepetopsis*, the shrimp *A. muricola* possessed  
370 depleted values of  $-35.5\text{‰}$  for *Provanna*,  $-48.8\text{‰}$  for the shrimps, and up to  $-55.0\text{‰}$  for the  
371 limpet specimens analysed, which suggests variable but a large contribution of bacteria in  
372 their diet, or different microbial communities with distinct signatures.  $\delta^{15}\text{N}$  of 3.28  
373 (*Alvinocaris*) to 3.89‰ (*Provanna*) are consistent with a trophic regimen of primary  
374 consumers, probably mainly based on microbial communities, considering a shift of 3.5 to

375 4‰ between prey and predator and a signature of archaeal and bacterial populations between  
376 -1‰ (mytilid methanotroph symbionts) and 1‰ (vesicomid sulphur-oxydising symbionts).  
377 The light signatures in carbon and nitrogen of *Paralepetopsis* collected at *Bathymodiolus*  
378 beds suggest a main consumption of methanotrophic Archaea. The turrid gastropod  
379 *Phymorrhynchus* has the same  $\delta^{13}\text{C}$  signature as the vesicomids, suggesting that bivalve  
380 tissues could partially be included in its diet. *Phymorrhynchus* has been observed in  
381 abundance among vesicomid clusters. Nevertheless, its  $\delta^{15}\text{N}$  values suggest another prey  
382 with a lighter signature. The echinoderms observed in the chemosynthetic assemblages such  
383 as *Chiridota* sp. or those close to them like the irregular echinoid, also have light  $\delta^{13}\text{C}$  values  
384 (respectively -57.1 and -41.3‰). Their  $\delta^{15}\text{N}$  values however differ, suggesting that echinids  
385 are primary consumers, probably grazing bacteria, while the holothurid has more enriched  
386 and more variable  $\delta^{15}\text{N}$  values suggestive of more recycling material in its diet. This species  
387 also could partially feed on bivalve tissues from which they have an enrichment of about 4.0-  
388 4.5‰ in  $\delta^{15}\text{N}$ . The detritivore/scavenger galatheids has nevertheless the most enriched  $\delta^{15}\text{N}$   
389 values (up to 9.7‰), corresponding to a higher trophic level. Finally, the zoarcid fish  
390 *Lycodes* sp. shows a quite variable signature in carbon (-25.4 to -68.0‰) and nitrogen  
391 (-1.23 to 9.4‰), probably revealing a fairly variable diet; some individuals were observed  
392 lying on bacterial mats while others are probably predators or scavengers of invertebrates.

393 Within some other species, especially *A. muricola* and *Chiridota* sp.,  $\delta^{13}\text{C}$  and  $\delta^{15}\text{N}$  values  
394 vary according to the sampling site. Signatures of shrimps collected on mussel beds show  
395 lighter values than those collected in vesicomid clusters (Figure 6a). These shrimps which  
396 have been observed grazing on bivalve mantles (Figure 6c) may have a nutritional link with  
397 bivalves, characterised by different isotopic signatures. The more variable  $\delta^{13}\text{C}$  signature of  
398 the shrimps at mytilid beds than at vesicomid beds may also correspond to a higher  
399 variability of microbe populations linked to methane- or sulphur-related processes. Similarly,

400 a difference between habitats has been observed for the holothurid, with a correspondence  
401 between  $\delta^{13}\text{C}$  values of the holothurid and of the dominant bivalves (mytilid/vesicomid)  
402 (Figure 6b). This species, which has been observed among bivalves (Figure 6c), could be a  
403 potential scavenger of bivalve tissues. Moreover, the very depleted value of its digestive wall  
404 ( $\delta^{13}\text{C} = -66.71\text{‰}$ ) compared with the tegument or tentacles (respectively  $-53.9$  and  $-55.1\text{‰}$ )  
405 may suggest the presence of bacteria in its digestive tract, although this was not seen by  
406 electronic microscope observations.

407

#### 408 3.3.4. Mobile megafauna collected by trawls

409 Twelve benthic or benthopelagic fish species were sampled in the trawls located from the  
410 REGAB site 14 km southward and northward. Some were collected only once or twice,  
411 others such as the *Acantaurus armatus* (Ophidiidae) were present in most of the trawl  
412 samples. Among the 11 species sampled close to the pockmark, 5 (*Coryphaenoides striatus*,  
413 *Stomias boa boa*, *Stylephorus chordatus*, *Bassozetus robustus* and *Porogadus milles*) were  
414 also collected at 4000-m sites and south of the Congo channel at 3000 m depth. The  
415 Ophidiidae (*A. armatus* and *B. robustus*) were the most abundant in trawls in the close  
416 vicinity of the seep area. *Lycodes* sp. (Zoarcidae) is the sole fish sampled only at the REGAB  
417 site, where it was observed by ROV among bivalve assemblages. Despite a strong  
418 heterogeneity in the isotopic signatures of the three specimens analysed, this species likely  
419 has a high percentage of chemosynthesis-originated carbon in its diet (35–100%) (Fig. 5,  
420 Table 7).

421 Among the other fishes sampled in the trawl hauls closest to the active area (CP19-20-21),  
422 the Ophidiidae *B. robustus*, *A. armatus* and *Holomycteronus squamosus* partially take  
423 advantage of this local production with a mean contribution of chemosynthesis-originated  
424 carbon from 15% for *A. armatus* to 38% for *H. squamosus* (Table 7). For some benthopelagic

425 fishes, *Scopeloberyx robustus* (Melamphaidae) and *Stylephorus chordatus* (Stylephoridae),  
426 the estimated percentage of chemosynthetic material is about 20%. Specimens of *Porogadus*  
427 *milles* showed variable signatures and the other species seem to be independent of the  
428 chemosynthetic production. A decrease in the chemosynthetic contribution to the fish diet  
429 with increasing distance from the pockmark was not observed, probably due to the large  
430 distribution perimeter of these individuals.

431 The two species of galatheids greatly differ in the isotopic signatures of their tissues and,  
432 therefore, by their dependence on the chemosynthetic production. Their distribution also  
433 appears to be different according to their distribution in trawls and as only *M. geyeri* was  
434 sampled during dives on REGAB.

435

#### 436 4. Discussion

437

##### 438 4.1. Level of dependence on chemosynthesis production

439

440 The distribution of the megafauna species along the dive tracks at the pockmark scale shows  
441 that the non-symbiont-bearing species, which are abundant within chemosynthetic  
442 assemblages (*A. muricola*, *Chiridota* sp.), are closely associated with symbiont-bearing  
443 species and as they are not, or rarely, observed outside the assemblages. *Phymorrhynchus*  
444 and the galatheids are mainly located in the periphery of the chemosynthetic assemblages but  
445 also do not have a regular distribution all over the pockmark, like fishes for example.  
446 Although few species can be included in such analysis based on video processing, there is  
447 evidence of the three levels of relationship, and possibly dependence, of the megafauna  
448 species relative to the seeps and chemoautotrophic processes, as defined by Carney (1994) as:  
449 endemic, colonists and vagrant species. *A. muricola* and *Chiridota* sp. may be more

450 dependent on the chemosynthetic production and may be endemic, whereas *Phymorrhynchus*  
451 and the galatheids may be colonists of the seep ecosystem. Carbon isotopic signatures of  
452 these two species are, moreover, less depleted than other heterotrophs sampled in the  
453 assemblages; this seems to confirm a lesser degree of chemosynthetic dependence than for *A.*  
454 *muricola* or *Chiridota* sp.. The small gastropods *Provanna* and *Paralepetopsis*, whose  
455 distribution of the chemosynthetic assemblages could not be estimated using video transects,  
456 are also probably strongly dependent on seep processes, judging from to their  $\delta^{13}\text{C}$  values.  
457 These two species were also abundant in chemosynthesis assemblages in the central active  
458 part of the pockmark (mytilid and vesicomylid beds, adult escarpiid bushes), but absent in the  
459 vesicomylid clusters located at the periphery of the pockmark, which was less active in terms  
460 of fluid emission.

461

#### 462 4.2. Trophic guilds and contribution to the biomass

463

464 Biomass of megafauna in chemosynthetic assemblages of the REGAB site is dominated by  
465 symbiont-bearing species. With the exception of *E. southwardae* which presents variability  
466 already observed for the Siboglinidae polychaetes (Conway et al., 1994; MacAvoy et al.,  
467 2005); all the other symbiont hosts have a homogeneous isotopic signature. The variability of  
468 the carbon isotopic signature according to the different sites, could be related to the use of  
469 different DIC sources (which might reflect different carbon signatures), to methane  
470 concentration and to the age of the tubeworm. However, at the well-studied Gulf of Mexico  
471 seeps, no differences between old and young tube-worm aggregations were observed for  
472 *Lamellibrachia luymesii* ( $-20\text{‰}$ ) and *Seepiophyla jonesi* ( $-22\text{‰}$ ) (MacAvoy et al., 2005). The  
473 mytilid *Bathymodiolus* sp. aff. *boomerang* possesses both methanotrophic and sulphur-  
474 oxidising symbionts (Duperron et al., 2005), but at the sites sampled for this study the carbon

475 isotopic signature of their tissues is very close to that of methane and mainly derives its  
476 carbon from methanotrophy according to the mixing equations applied to our stable isotope  
477 measurements. The most depleted  $\delta^{13}\text{C}$  values, suggesting a higher contribution of  
478 methanotrophic symbionts, originated from the M2 site mytilids where the highest methane  
479 concentrations were recorded. This situation is closer to that of mussels in the Gulf of Mexico  
480 seeps that have only methanotrophic symbionts (Brooks et al., 1987) than that of the Blake  
481 ridge mussels *Bathymodiolus heckeriae*, which, like REGAB mytilids, harbour two types of  
482 symbionts (Van Dover et al., 2003). The vesicomyids and *E. southwardae* harbour only  
483 sulphur-oxidising bacteria (Nadalig et al., in press). After symbiont-bearing species, the  
484 second contributor to the biomass is the shrimp *A. muricola*, representing up to 10% of the  
485 total dry weight of mytilid and vesicomyid clusters (M1, VC), and 25 % in the tube-worm  
486 aggregations. Densities reach 450ind.m<sup>-2</sup> in mussel beds. In contrast, they show low densities  
487 in some vesicomyid clusters of peripheral areas (V1, Vext). According to its nitrogen isotopic  
488 signature, the shrimp seems to be mainly a primary consumer. Similarly, in the Gulf of  
489 Mexico seeps, *Alvinocaris stactophila* was one of the most abundant species associated with  
490 mussel beds, accounting for up to 17% of the individuals collected, apart from mussels, and  
491 this species being related to the higher methane concentrations (Bergquist et al., 2005), which  
492 is consistent with our observations. Other primary consumers mainly relying on microbial  
493 biomass (*Provanna.*, *Paralepetopsis*) may have very high densities, equivalent to those of  
494 shrimps in most of the bivalves clusters, and sometimes higher (at M1); however the biomass  
495 is much less owing to their small size. Quantitative sampling could, nevertheless, give  
496 slightly different results, with image analysis biased toward the larger species. Small  
497 gastropods are also the most abundant species in Gulf of Mexico mussel beds, with *Provanna*  
498 *sculpta* accounting for up to 14% of the individuals (Bergquist et al. 2005). Echinids are not  
499 included in density/biomass estimation as they are mainly located in the vicinity of the

500 chemosynthetic assemblages. Nevertheless, they are abundant in soft sediment areas close to  
501 vesicomid beds and are another species that seem to be mainly primary consumers of  
502 microbial chemoautotrophic communities.

503 Higher trophic levels including the holothurid, galatheids and zoarcid fish are not very  
504 abundant in the sampled assemblages, except locally for *Chiridota* sp. in bivalve beds (93  
505 ind.m<sup>-2</sup> and 5% of the biomass in V3), which could be a scavenger of both vesicomids and  
506 mussels. The density and biomass of these higher trophic levels (detritivorous, scavengers,  
507 predators) increase with the proportion of empty shells in vesicomid clusters, *M. geyeri* and  
508 *Phymorrhynchus* in V1, *Chiridota* (11 ind/m<sup>2</sup>), *Phymorrhynchus* and *M. geyeri* in VB. At the  
509 pockmark scale, distribution based on transects show that holothurids and galatheids are quite  
510 abundant in the area colonised by chemosynthesis-based communities (Fig. 3). Galatheids  
511 belonging to the genus *Munidopsis* have been reported to be dependent on chemosynthetic  
512 production at deep seeps (Levin and Michener, 2002) and to feed on vesicomid clams  
513 (Sahling et al., 2003). At the REGAB site their  $\delta^{15}\text{N}$  signature suggests a diet mainly based  
514 on recycled material. Low predation pressure in living chemosynthetic assemblages has been  
515 suggested at deep cold-seep sites compared with shallower sites (Sahling et al. 2003).  
516 Nevertheless, *Phymorrhynchus* observed in abundance in some vesicomid clusters,  
517 particularly in the periphery areas, may not only be a scavenger but also an active predator  
518 (A. Warén, pers. com.).

519 The primary “consumers”, via endosymbioses with chemoautotrophic bacteria, or mainly  
520 grazing on free-living microbial communities, therefore dominate the chemosynthetic  
521 assemblages in the active centre of the pockmark. There are some possible  
522 predators/scavengers, but their densities and biomass are low, at least in the assemblages  
523 sampled for this study. In the periphery, the low-density vesicomid clusters with a high  
524 proportion of empty shells provide detrital material for detritivores and scavengers, and

525 higher trophic levels dominate the heterotrophic fauna. Such a community structure, with a  
526 clear dominance of primary consumers, symbiont hosts and bacterivores, has been observed  
527 from quantitative sampling in the hydrothermal vent community dominated by the siboglinid  
528 *Ridgeia piscesae* (Bergquist et al., 2007). The commensal Polynoidae *Branchipolynoe* sp. has  
529 been found in most of the mussels collected on REGAB but the sampling effort is not  
530 sufficient to estimate its abundance, and it could represent a non-negligible part of the  
531 biomass. As observed in other hydrothermal vent and cold-seep sites, its isotopic signature  
532 suggests a strong nutritional relationship with its host (Colaço et al., 2002; Fisher et al., 1994;  
533 Suzuki et al., 1989; Van Dover et al., 2003). According to Desbruyères et al. (1985) from gut  
534 content analyses, commensal polynoids nutrition is based on mussel mucus-rich pseudo-  
535 faeces and gills. More generally, the polychaete community that is not included in this study,  
536 likely play an important role in the community structure and could contribute to the biomass  
537 of predators, as has been shown in hydrothermal vent communities for polynoids in particular  
538 (Bergquist et al. 2007). At seeps, the Amphinomid polychaete has been suggested to obtain  
539 significant dietary carbon directly from the symbiont-containing *Bathymodiolus childressi*  
540 (MacAvoy et al. 2005).

541 Finally, biomass of associated species is highest in mytilid beds and more variable in  
542 vesicomid clusters, mostly due to the presence or absence of only one species *Chiridota* sp.  
543 Nevertheless, the infauna that are not included in this study probably contribute more to the  
544 biomass than in the case of mytilid and siboglinids.

545

#### 546 4.3. Transfer of seep organic matter to the surrounding ecosystem

547

548 The mobile benthic predators/scavengers that use chemosynthetic biomass may contribute to  
549 the export of seep organic production to the surrounding ecosystem. Isotopic measurements  
550 suggest that the contribution of chemosynthetic material in fish diet is variable among the

551 species but not negligible (more than 15% and up to 38%) for 5 of the species captured off  
552 the cold-seep site among the 12 analysed. These species have been sampled at least in the  
553 northern part of the cold-seep site (CP20) or in a 100-m radius around the pockmark and  
554 some (Ophidiidae) have been observed during ROV dives. Only the Zoarcidae *Lycodes* sp. is  
555 resident in the seeps, and may be endemic, according to its high degree of dependence from  
556 chemosynthetic production and their absence in trawl samples outside the seep site. The two  
557 species of galatheids differ greatly in the isotopic signatures of their tissues and, therefore, by  
558 their dependence on the chemosynthetic production. Their distribution also appears to be  
559 different according to their distribution in trawls and as only *M. geyeri* was sampled during  
560 dives on REGAB.

561 In comparison, a similar study in the shallower sites of the Gulf of Mexico (MacAvoy et al.  
562 2002) showed several species of fish and invertebrates that obtained between 50 and 100% of  
563 their nutrition from seep production, indicating that they are resident to the seeps. There is  
564 also a greater abundance of vagrants at bathyal depths than at 3200 m depth. MacAvoy et al.  
565 indicated that several vagrant predators/scavengers sampled on seep sites, including fishes  
566 (*Nezumia* sp., *Oligopus* sp., and the eels *Synaphobranchus* sp., *Ophichthus cruentifer* and  
567 *Dysomma rugosa*) and three invertebrates (*Bathynomus giganteus*, *Buccinum canetae*,  
568 *Scleracterias tanneri*) have a significant contribution of chemosynthetic material in their diet.  
569 Predation by large and mobile species of seep resident species is probably much higher at  
570 these shallow sites, because the surrounding benthos is probably more depauperate, as  
571 suggested by Sahling et al. (2003) in the Sea of Okhotsk. However, all these species were  
572 captured on the Louisiana slope cold-seep sites whereas those collected off-site by traps (2  
573 km from the location of the seep communities) used from 0 to 40% of chemosynthetic  
574 material, which is not different from our study.

575

576 4.4. Comparison with other cold-seep communities in the Atlantic

577

578 The chemosynthetic assemblages of the REGAB site share many genera and even species  
579 with other cold-seep sites in the Atlantic. The alvinocarid shrimp *Alvinocaris muricola* has  
580 been collected in the Gulf of Mexico (Carney, 1994; Cordes et al., 2007), Blake Ridge (Van  
581 Dover et al. 2003) and Barbados seep aggregations (Olu et al., 1996), and the chirodotid  
582 holothurian *Chiridota heveva*, which seems to be very close to the REGAB species, was first  
583 described from the Blake Ridge mussel beds (Pawson and Vance, 2004). The gastropod  
584 *Provanna sculpta* is abundant within Gulf of Mexico mussel beds (Bergquist et al., 2005) and  
585 tube-worm aggregations (Bergquist et al., 2003). Actinians have also been reported in Blake  
586 Ridge mussel beds and from the Florida escarpment (Cordes et al., 2007; Van Dover et al.,  
587 2003). Galatheid crabs *Munidopsis* sp. are generally associated. The commensal polynoid  
588 *Branchipolynoe seepensis* may also be a common species to West Atlantic and East Atlantic  
589 cold-seep mussels (Desbruyères and Hourdez, unpubl.) The community inhabiting the  
590 REGAB pockmark is very similar to the group of communities described for the deep seeps  
591 of the Gulf of Mexico (2200–3300 m), the intermediate-depth sites of the Barbados prism  
592 (1700–2000) and the 2150 m Blake Ridge sites, which have been included in the same group,  
593 clustered by depth instead of geography by Cordes et al. (2007). Indeed this ‘deep’ seep  
594 community from the western Atlantic includes *E. laminata* and *B. heckerae* or *B. boomerang*  
595 as structuring species, and *A. muricola*, *Munidopsis* sp., *B. seepensis*, *Chiridota* sp.,  
596 *Phymorrhynchus* sp. a Nautillinellid polychaete and the ophiurid *Ophioctenella acies*. Except  
597 for these last two species, all the other species or genera have been sampled on REGAB.  
598 Most intriguing is the co-occurrence of similar species from both sides of the Atlantic, that  
599 has been discussed for *Bathymodiolus boomerang* (Olu-Le Roy et al. 2007b) as example of  
600 two amphi-atlantic Bathymodiolinae species complexes, Alvinocarid shrimps (Komai and

601 Segonzac 2005), and more generally by Cordes et al. (2007) comparing associated fauna  
602 from box core sampling on the Nigerian margin and cold-seep communities from the Eastern  
603 Atlantic.

604

## 605 5. Conclusion

606 The REGAB pockmark cold-seep community is the first to be described in the Equatorial  
607 East Atlantic and the second in the Eastern Atlantic after the Haakon Mosby Mud Volcano  
608 located in high latitudes (Gebruk et al. 2003). REGAB's striking feature is the abundance and  
609 diversity of large symbiont-bearing species, mytilid and vesicomid bivalves and siboglinids,  
610 forming puzzling habitats hosting chemosynthetic assemblages, whose highest biomasses are  
611 found in the mussel beds likely located in the highest fluid flow areas. Associated megafauna  
612 is very similar among assemblage types, with few same dominant taxa but whose individuals  
613 may be closely associated with local aggregates as suggested by the variation of isotopic  
614 signatures according to the types of aggregates or habitat. These associate species, which are  
615 likely endemics of the seep community, mainly use chemosynthesis-derived carbon but with  
616 variable contribution of methanotrophy or thiotrophy. Biomass in the sampled assemblages  
617 was dominated by primary "consumers", either symbiont-bearing species or feeders of free  
618 living microbes, such as shrimps or gastropods. Scavengers (galatheids, probably  
619 holothurids) and possible predators (*Phymorhynchus* and zoarcid fishes) representing the  
620 higher trophic levels are less dense distributed but occur all over the area colonised by  
621 chemosynthetic assemblages. Export of local production by colonists or vagrant species is  
622 reduced compared to shallower depth seeps but has been shown for 7 species of fish with  
623 more than 10% contribution of chemosynthesis-based carbon and for two galatheids. The  
624 REGAB community bears a high resemblance to those associated with seeps in the western  
625 Atlantic (Barbados prism, Gulf of Mexico, Blake Ridge). Further sampling efforts using

626 quantitative tools are necessary to describe better the communities associated with each of the  
627 three chemosynthetic assemblages, and for comparison with studies on similar habitats in the  
628 Gulf of Mexico seeps. The REGAB pockmark is an unusual cold-seep site by the high spatial  
629 heterogeneity of habitats in a relatively restricted area, which makes comparisons easier  
630 between habitats and chemosynthetic assemblages. Thus it is possible to identify the factors  
631 controlling the community structure without the influence of factors that may play a role in a  
632 broader scale, such as bathymetry, geology of the structures, or biogeography.

633

634

635

#### 636 Acknowledgements

637 The BIOZAIRE program was partially funded by TOTAL (P.I. M. Sibuet for Ifremer). We are  
638 grateful to the chief scientists of the BIOZAIRE 1, 2 and 3 cruises (M. Sibuet, A.  
639 Khrippounoff), and to the captains and the crews of the N.O. L'Atalante and VICTOR 6000  
640 team. We are indebted to A. Fifis who processed the samples processing during the  
641 BIOZAIRE 2 cruise and M.-C. Fabri for her useful help particularly for the database  
642 management (BIOCEAN). All our colleagues on the Biozaire 2 and 3 cruises are thanked for  
643 their help onboard. A. Le Goff and A. Bousquet contributed to sample processing. A. Warén  
644 is thanked for discussions about nutritional strategies of gastropods. We are indebted to the  
645 anonymous reviewers for their helpful comments and suggestions to improve the manuscript.  
646 We are grateful to Myriam Sibuet and Annick Vangriesheim for the co-edition of this special  
647 issue on the Biozaire program. This work contributes to the Census of Marine Life project  
648 COMARGE (Continental Margin Ecosystems on a worldwide scale).

649

#### 650 References

- 651 Barry, J.P., Kochevar, R.E., Baxter, C.H., 1997. The influence of pore-water chemistry and  
652 physiology in the distribution of vesicomimid clams at cold seeps in Monterey Bay :  
653 implications for patterns of chemosynthetic community organization. *Limnology and*  
654 *Oceanography* 42 (2), 318-328.
- 655 Bergquist, D.C., Eckner, J.T., Urcuyo, I.A., Cordes, E.E., Hourdez, S., Macko, S.A., Fisher,  
656 C.R., 2007. Using stable isotopes and quantitative community characteristics to determine  
657 a local hydrothermal vent food web. *Marine Ecology Progress Series* 330, 49-65.
- 658 Bergquist, D.C., Fleckenstein, C., Knisel, J., Begley, B., MacDonald, I.R., Fisher, C.R., 2005.  
659 Variations in seep mussel bed communities along physical and chemical environmental  
660 gradients. *Marine Ecology Progress Series* 293, 99-108.
- 661 Bergquist, D.C., Ward, T., Cordes, E.E., McNelis, T., Howlett, S., Kosoff, R., Hourdez, S.,  
662 Carney, R., Fisher, C.R., 2003. Community structure of vestimentiferan-generated habitat  
663 islands from Gulf of Mexico cold seeps. *Journal of Experimental Marine Biology and*  
664 *Ecology* 289, 197-222.
- 665 Brooks, J.M., Kennicutt II, M.C., Fisher, C.R., Macko, S.A., Cole, K., Childress, J.J.,  
666 Bidigare, R.R., Vetter, R.D., 1987. Deep-sea hydrocarbon seep communities: Evidence  
667 for energy and nutritional carbon sources. *Science* 238, 1138-1142.
- 668 Cambon Bonavita, M., Nadalig, T., Roussel, E., Delage, E., Duperron, S., Caprais, J.C.,  
669 Boetius, A., Sibuet, M., 2009. Distribution of AOM aggregates and microbial diversity  
670 associated to different faunal assemblages in a giant pockmark of Gabon continental  
671 margin. *Deep Sea Research II* (this volume).
- 672 Carney, R.S., 1994. Consideration of the oasis analogy for chemosynthetic communities at  
673 Gulf of Mexico hydrocarbon vents. *Geo-Marine Letters* 14, 149-159.
- 674 Charlou, J.L., Donval, J.P., Fouquet, Y., Ondreas, H., Knoery, J., Cochonat, P., Levache, D.,  
675 Poirier, Y., Jean-Baptiste, P., Fourre, E., 2004. Physical and chemical characterization of  
676 gas hydrates and associated methane plumes in the Congo-Angola Basin. *Chemical*  
677 *Geology* 205 (3-4), 405.
- 678 Colaço, A., Dehairs, F., Desbruyères, D., 2002. Nutritional relations of deep-sea  
679 hydrothermal fields at the Mid-Atlantic Ridge: a stable isotope approach. *Deep-Sea*  
680 *Research* 49, 395-412.
- 681 Conway, N.M., Kennicutt, M.C., Van Dover, C.L., 1994. Stable isotopes in the study of  
682 marine chemosynthetic-based ecosystems. Blackwell scientific publications, London.
- 683 Cordes, E.E., Carney, S.L., Hourdez, S., Carney, R.S., Brooks, J.M., Fisher, C.R., 2007. Cold  
684 seeps of the deep Gulf of Mexico: Community structure and biogeographic comparisons  
685 to Atlantic equatorial belt seep communities. *Deep Sea Research Part I: Oceanographic*  
686 *Research Papers* 54 (4), 637-653.
- 687 Cordes, E.E., Hourdez, S., Predmore, B.L., Redding, M.L., Fisher, C.R., 2005. Succession of  
688 hydrocarbon seep communities associated with the long-lived foundation species  
689 *Lamellibrachia luymesi*. *Marine Ecology Progress Series* 305, 17-29.
- 690 Cosel, R.von, Olu, K., 2008. A new genus and new species of Vesicomiyidae (Mollusca:  
691 Bivalvia) from cold seeps on the Barbados accretionary prism, with comments on other  
692 species. *Zoostystema* 30 (4): 929-944

- 693 Cosel, R.von, Olu, K., in press. Large Vesicomidae (Mollusca: Bivalvia) from cold seeps in  
694 the Gulf of Guinea off the coasts of Gabon, Congo and northern Angola. Deep Sea  
695 Research II (this volume).
- 696 Desbruyères, D., Gaill, F., Laubier, L., Fouquet, Y., 1985. Polychaetous annelids from  
697 hydrothermal vent ecosystems: An ecological overview. Bull. Biol. Soc. Wash. 6, 103-  
698 116.
- 699 Duperron, S., Nadalig, T., Caprais, J.C., Sibuet, M., Fiala-Médioni, A., Amann, R., Dubilier,  
700 N., 2005. Dual symbiosis in a Bathymodiulus sp mussel from a methane seep on the  
701 gabon continental margin (southeast Atlantic): 16S rRNA phylogeny and distribution of  
702 the symbionts in gills. Applied and Environmental Microbiology 71 (4), 1694-1700.
- 703 Fisher, C.R., Childress, J.J., Macko, S.A., Brooks, J.M., 1994. Nutritional interactions in  
704 Galapagos Rift hydrothermal vent communities: inferences from stable carbon and  
705 nitrogen isotope analyses. Marine Ecology Progress Series 103, 45-55.
- 706 Fry, B., Sherr, E.B., 1984.  $\delta^{13}\text{C}$  measurements as indicators of carbon flow in marine and  
707 freshwater ecosystems. Contributions in Marine Science 27, 13-47.
- 708 Gebruk, A., Krylova, E.M., Lein, A., Vinogradov, G.M., Anderson, E., Pimenov, N.V.,  
709 Cherkashev, G.A., Crane, K., 2003. Methane seep community of the Hakon Mosby mud  
710 volcano the Norwegian Sea: composition and trophic aspects. Sarsia 88 (6), 394-403.
- 711 Henry, P., Foucher, J.P., Le Pichon, X., Sibuet, M., Kobayashi, K., Tarits, P., Chamot-Rooke,  
712 N., Furuta, T., Schultheiss, P., 1992. Interpretation of temperature measurements from the  
713 Kaiko-Nankai cruise: Modeling of fluid flow in clam colonies. Earth and Planetary  
714 Science Letters 109, 355-371.
- 715 Kennicutt II, M.C., Burke Jr., R.A., Mac Donald, I.R., Brooks, J.M., Denoux, G.J., Macko,  
716 S.A., 1992. Stable isotope partitioning in seep and vent organisms: chemical and  
717 ecological significance. Chemical Geology (Isotope Geosciences Section) 101, 293-310.
- 718 Komai, T., Segonzac, M., 2005. A revision of the genus *Alvinocaris* Williams and Chace  
719 (Crustacea: Decapoda: Caridea: Alvinocaridea), with descriptions of a new genus and a  
720 new species of *Alvinocaris*. Journal of Natural History 39 (15), 1111-1175.
- 721 Levesque, C., Juniper, K., Marcus, J., 2003. Food resource partitioning and competition  
722 among alvinellid polychaetes of Juan de Fuca Ridge hydrothermal vents. Marine Ecology  
723 Progress Series 246, 173-182.
- 724 Levesque, C., Kim Juniper, S., Limen, H., 2006. Spatial organization of food webs along  
725 habitat gradients at deep-sea hydrothermal vents on Axial Volcano, Northeast Pacific.  
726 Deep Sea Research Part I: Oceanographic Research Papers In Press, Corrected Proof.
- 727 Levin, L.A., 2005. Ecology of cold seep sediments: interactions of fauna with flow,  
728 chemistry and microbes. Oceanography and Marine Biology Annual Review 43, 1-46.
- 729 Levin, L.A., James, D.W., Martin, C.M., Rathburn, A., Harris, L., Michener, R., 2000. Do  
730 methane seeps support distinct infaunal assemblages? Observations on community  
731 structure and nutrition from the northern California slope and shelf. Marine Ecology  
732 Progress Series 208, 21-39.
- 733 Levin, L.A., Michener, H.M., 2002. Isotopic evidence for chemosynthesis-based nutrition of  
734 macrobenthos: The lightness of being at Pacific methane seeps. Limnology and  
735 Oceanography 47 (5), 1336-1345.

- 736 Levin, L.A., Ziebis, W., Mendoza, G.F., Growney, V.A., Tryon, M.D., Mahn, C., Gieskes,  
737 J.M., Rathburn, A.E., 2003. Spatial heterogeneity of macrofauna at northern California  
738 methane seeps: influence of sulfide concentration and fluid flow. *MEPS* 265, 123-139.
- 739 MacAvoy, S.E., Carney, R.S., Fisher, C.R., Macko, S.A., 2002. Use of chemosynthetic  
740 biomass by large, mobile, benthic predators in the Gulf of Mexico. *Marine Ecology*  
741 *Progress Series* 225, 65-78.
- 742 MacAvoy, S.E., Fisher, C.R., Carney, R.S., Macko, S.A., 2005. Nutritional associations  
743 among fauna at hydrocarbon seep communities in the Gulf of Mexico. *Marine Ecology*  
744 *Progress Series* 292, 51-60.
- 745 MacDonald, I.R., Sager, W.W., Peccini, M.B., 2003. Gas hydrate and chemosynthetic biota  
746 in mounded bathymetry at mid-slope hydrocarbon seeps: Northern Gulf of Mexico.  
747 *Marine Geology* 198, 133-158.
- 748 Macpherson, E., Segonzac, M., 2005. Species of the genus *Munidopsis* (Crustacea,  
749 Decapoda, Galatheidae) from the deep Atlantic Ocean, including cold-seep and  
750 hydrothermal vent areas. *Zootaxa*, 1-60.
- 751 Micheli, F., Peterson, C.H., Mullineaux, L.S., Fisher, C.R., Mills, S., Sancho, G., Johnson,  
752 G.A., Lenihan, H.S., 2002. Predation structures communities at deep-sea hydrothermal  
753 vents. *Ecological Monographs* 72, 365-382.
- 754 Minegawa, M., Wada, E., 1984. Stepwise enrichment of <sup>15</sup>N along food chains: further  
755 evidence and the relation between <sup>15</sup>N and animal age. *Geochimical and Cosmochimical*  
756 *Acta* 48, 1135-1140.
- 757 Olu-Le Roy, K., Caprais, J.C., Fifis, A., Fabri, M.C., Galéron, J., Budzinski, H., Le Ménach,  
758 K., Khripounoff, A., Ondréas, H., Sibuet, M., 2007a. Cold seep assemblages on a giant  
759 pockmark off West Africa: spatial patterns and environmental control. *Marine Ecology*  
760 28, 115-130.
- 761 Olu-Le Roy, K., Cosel, R.v., Hourdez, S., Carney, S.L., Jollivet, D., 2007b. Amphi-Atlantic  
762 cold-seep *Bathymodiolus* species complexes across the equatorial belt. *Deep Sea*  
763 *Research Part I: Oceanographic Research Papers* 54 (11), 1890-1911.
- 764 Olu - Le Roy, K., Le Goff, A., Fifis, A., Caprais, J.C., Budzinsky, H., Le Ménach, K.,  
765 Khripounoff, A., Sibuet, M., in prep. Community structure and nutritional patterns of  
766 megafauna assemblages on a giant pockmark in the Gulf of Guinea.
- 767 Olu, K., Lance, F., Sibuet, M., Henry, P., Fiala-Médioni, A., Dinét, A., 1997. Cold seep  
768 communities as indicators of fluid expulsion patterns through mud volcanoes seaward of  
769 the Barbados accretionary prism. *Deep-Sea Research I* 44 (5), 811-841.
- 770 Olu, K., Sibuet, M., Harmegnies, F., Foucher, J.-P., Fiala-Medioni, A., 1996. Spatial  
771 distribution of diverse cold seep communities living on various diapiric structures of the  
772 southern Barbados prism. *Progress in Oceanography* 38, 347-376.
- 773 Ondréas, H., Olu, K., Fouquet, Y., Charlou, J., Gay, A., Dennielou, B., Donval, J., Fifis, A.,  
774 Nadalig, T., Cochonat, P., Cauquil, E., Bourillet, J., Moigne, M., Sibuet, M., 2005. ROV  
775 study of a giant pockmark on the Gabon continental margin. *Geo-Marine Letters* 25 (5),  
776 281.
- 777 Paull, C.K., Hecker, B., Commeau, R., Freeman-Lynde, R.P., Neumann, C., Corso, W.P.,  
778 Golubic, S., Hook, J.E., Sikes, E., Curray, J., 1984. Biological communities at the Florida  
779 escarpment resemble hydrothermal vent taxa. *Science* 226, 965-967.

- 780 Paull, C.K., Jull, A.J.T., Toolin, L.J., Linick, T., 1985. Stable isotope evidence for  
781 chemosynthesis in an abyssal seep community. *Nature*, pp. 709-711.
- 782 Pawson, D.L., Vance, D.J., 2004. *Chirodota heheva*, new species, from Western Atlantic  
783 deep-sea cold seeps and anthropogenic habitats (Echinodermata: Holothuroidea:  
784 Apodida). *Zootaxa* 534, 1-12.
- 785 Polz, M.F., Robinson, J.J., Cavanaugh, C.M., Van Dover, C.L., 1998. Trophic ecology of  
786 massive shrimp aggregations at a Mid-Atlantic Ridge hydrothermal vent site. *Limnology  
787 and Oceanography* 43 (7), 1631-1638.
- 788 Rau, G.H., Hedges, J.I., 1979. Carbon-13 depletion in a hydrothermal vent mussel:  
789 suggestion of a chemosynthetic food source. *Science* 203, 648-649.
- 790 Rau, G.H., Mearns, A.J., Young, D.R., Olsen, R.J., Schafer, H.A., Kaplan, I.R., 1983. Animal  
791  $^{13}\text{C}/^{12}\text{C}$  correlates with trophic levels in pelagic food webs. *Ecology* 64, 1314-1318.
- 792 Sahling, H., Galkin, S.V., Salyuk, A., Greinert, J., Foerstel, H., Piepenburg, D., Suess, E.,  
793 2003. Depth-related structure and ecological significance of cold-seep communities--a  
794 case study from the Sea of Okhotsk. *Deep Sea Research Part I: Oceanographic Research  
795 Papers* 50 (12), 1391-1409.
- 796 Sahling, H., Rickert, D., Lee, R.W., Linke, P., Suess, E., 2002. Macrofaunal community  
797 structure and sulfide flux at gas hydrate deposits from the Cascadia convergent margin,  
798 NE Pacific. *Marine Ecology Progress Series* 231, 121-138.
- 799 Sarrazin, J., Juniper, K., 1999. Biological characteristics of a hydrothermal edifice mosaic  
800 community. *Marine Ecology Progress Series* 185, 1-19.
- 801 Sarrazin, J., Juniper, S.K., Massoth, G., Legendre, P., 1999. Physical and Chemical factors  
802 influencing species distributions on hydrothermal sulfide edifices of the Juan de Fuca  
803 Ridge, Northeast Pacific. *Marine Ecology Progress Series* 190, 89-112.
- 804 Sibuet, M., Olu-Le Roy, K., 2002. Cold Seep Communities on Continental Margins:  
805 Structure and Quantitative Distribution Relative to Geological and Fluid Venting  
806 Patterns. In: G. Wefer, D.B., D. Hebbeln, B.B. Jorgensen, T. Van Weering (Ed.), *Ocean  
807 Margin Systems*. Springer Verlag, Berlin, pp. 235-251.
- 808 Sibuet, M., Olu, K., 1998. Biogeography, biodiversity and fluid dependence of deep-sea cold-  
809 seep communities at active and passive margins. *Deep-Sea Research II* 45, 517-567.
- 810 Sibuet M, Vangriesheim A (2009) Deep-Sea Environment and Biodiversity of the West  
811 African Equatorial margin. *Deep Sea Research II* this volume
- 812 Suzuki, T., Takagi, T., Ohta, S., 1989. Primary structure of a dimeric haemoglobin from the  
813 deep-sea cold-seep clam *Calyptogena soyoeae*. *Biochemical Journal* 260, 177-182.
- 814 Thiele, J., Jaeckel, S., 1931. Muscheln der Deutschen Tiefsee-Expedition. *Wissenschaftliche  
815 Ergebnisse der Deutschen Tiefsee-Expedition auf dem Dampfer "Valdivia"* 21(1), 159-  
816 268, 5 pls: Gustav Fischer, Jena.
- 817 Tunnicliffe, V., 1991. The biology of hydrothermal vents : ecology and evolution. In: Barnes,  
818 M. (Ed.), *Oceanogr. Mar. Biol. Annu. Rev.* Aberdeen University Press, pp. 319-407.
- 819 Van Dover, C., Aharon, P., Bernhard, J.M., Caylor, E., Doerries, M., Flickinger, W.,  
820 Gilhooly, W., Goffredi, S.K., Knick, K., Macko, S.A., Rapoport, S., Raulfs, E.C., Ruppel,  
821 C., Salerno, J., Seitz, R.D., Sen Gupta, B.K., Shank, T., Turneipseed, M., Vrijenhoek,  
822 R.C., 2003. Blake Ridge methane seep: characterization of a soft-sediment,  
823 chemosynthetically based ecosystem. *Deep-Sea Research I* 50, 281-300.

824 Van Dover, C.L., 1995. Ecology of Mid-Atlantic Ridge hydrothermal vents. In: Parson, L.M.,  
825 Walker, C.L., Dixon, D.R. (Eds.), Hydrothermal vents and processes. Geological Society  
826 Special Publication, London, pp. 257-294.

827 Van Dover, C.L., 2002. Trophic relationships among invertebrates at the Karei hydrothermal  
828 vent field (Central Indian Ridge). *Marine Biology* 141, 761-772.

829 Van Dover, C.L., Fry, B., 1989. Stable isotopic compositions of hydrothermal vent  
830 organisms. *Marine Biology* 102, 257-263.

831 Vereshchaka, A.L., Vinogradov, G.M., Lein, A.Y., Dalton, S., Dehairs, F., 2000. Carbon and  
832 nitrogen isotopic composition of the fauna from the Broken Spur hydrothermal vent field.  
833 *Marine Biology* 136, 11-17.

834 Warén, A., Bouchet, P., in press. New gastropods from deep-sea hydrocarbon seeps off West  
835 Africa. *Deep Sea Research II*.

836

837

838 Table and figure caption

839

840 Table 1: Characteristics of the sampling sites based on dominant symbiont-bearing species.

841 Abbreviations: Mx: site dominated by Mytilidae; Vx: by Vesicomidae, E: by  
842 Escarpiidae. For the location, see Fig.2b.

843

844 Table 2: Densities (ind.m<sup>-2</sup>) (a) and biomass (g dry weight.m<sup>-2</sup>) (b) of megafauna species from

845 image analysis and sampling in the clusters defined by symbiont bearing species (M:

846 clusters dominated by mytilids; V: by vesicomids, E: by escarpiids). n.e.: non

847 estimated

848

849 Table 3: Isotopic carbon signature ( $\delta^{13}\text{C}$ ) of methane extracted from sediment or expelled

850 fluid on the REGAB pockmark. Percentage of methane in the total gas fraction is

851 calculated from gas chromatography peak integration.

852

853 Table 4: Isotopic signatures of sediment and particles sampled by cores or traps in and off the

854 REGAB pockmark.

855

856 Table 5: Isotopic signatures of symbiont-bearing species from different sampling sites in the

857 REGAB pockmark.

858

859 Table 6: Mean isotopic signatures of associated megafauna sampled by ROV in the clusters  
860 dominated either by mytilids (M), vesicomyids (V) or escarpiids (E) or by trawl  
861 (CP20) in the REGAB cold-seep site.

862

863 Table 7: Isotopic signature ( $\delta^{13}\text{C}$ ) of fishes sampled by trawls at increasing distance from the  
864 REGAB site and estimated percentages of chemosynthetic material in their diet. See  
865 fig. 1 for the localization of trawls.

866

867 Figure 1: Location of the REGAB pockmark along the Congo-Angola margin and of the  
868 benthic trawls

869

870 Figure 2:a. Location of the dive tracks in the REGAB site, analyzed for megafauna  
871 distribution, and of sampling sites. Two dive tracks are represented by the black and  
872 grey lines; the box indicates the area surveyed by five more dives. b. Distribution of  
873 chemosynthetic assemblages along the dive tracks, classified by the dominance of  
874 symbiotic species (from Olu-Le Roy et al. 2007a).

875

876 Figure 3: Distribution maps of major associated megafauna species along the dive tracks. a.  
877 *Chiridota* sp., b. *Munidopsis* sp., c. *Alvinocaris muricola*, d. Irregular echinid.

878

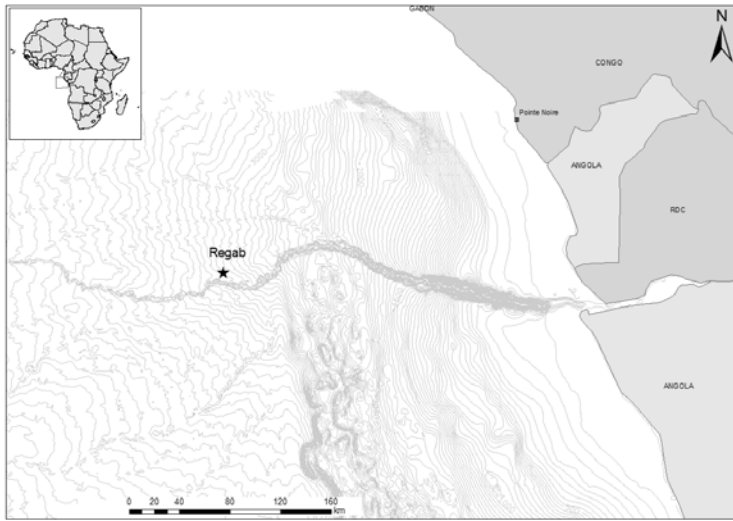
879 Figure 4: Multidimensional scaling (MDS) plots of the species/biotope matrix of distance  
880 using the Bray Curtis distance (Primer software). **a.** Similarity between biotopes, **b.**  
881 Similarity between species. H=hydrate outcrop, B=gas bubbles, BM=bacterial mat,  
882 Conc=carbonate concretion, S= soft sediment, RS=reduced sediment, Ed=dead  
883 escarpiids, El=live escarpiids, M=mytilids, Vd=dead vesicomyids, Vl=live  
884 vesicomyids, Vm=mixed (live and dead) vesicomyids.

885

886 Figure 5: Mean  $\delta^{13}\text{C}$  vs  $\delta^{15}\text{N}$  values of each species, sediment samples or particles analysed  
887 from the REGAB pockmark. The signatures of the three Zoarcidae fish are  
888 represented to show the high variability between specimens. Methane  $\delta^{13}\text{C}$  values are  
889 also plotted. CI to CIII correspond to the different levels of consumers (from primary  
890 to tertiary)

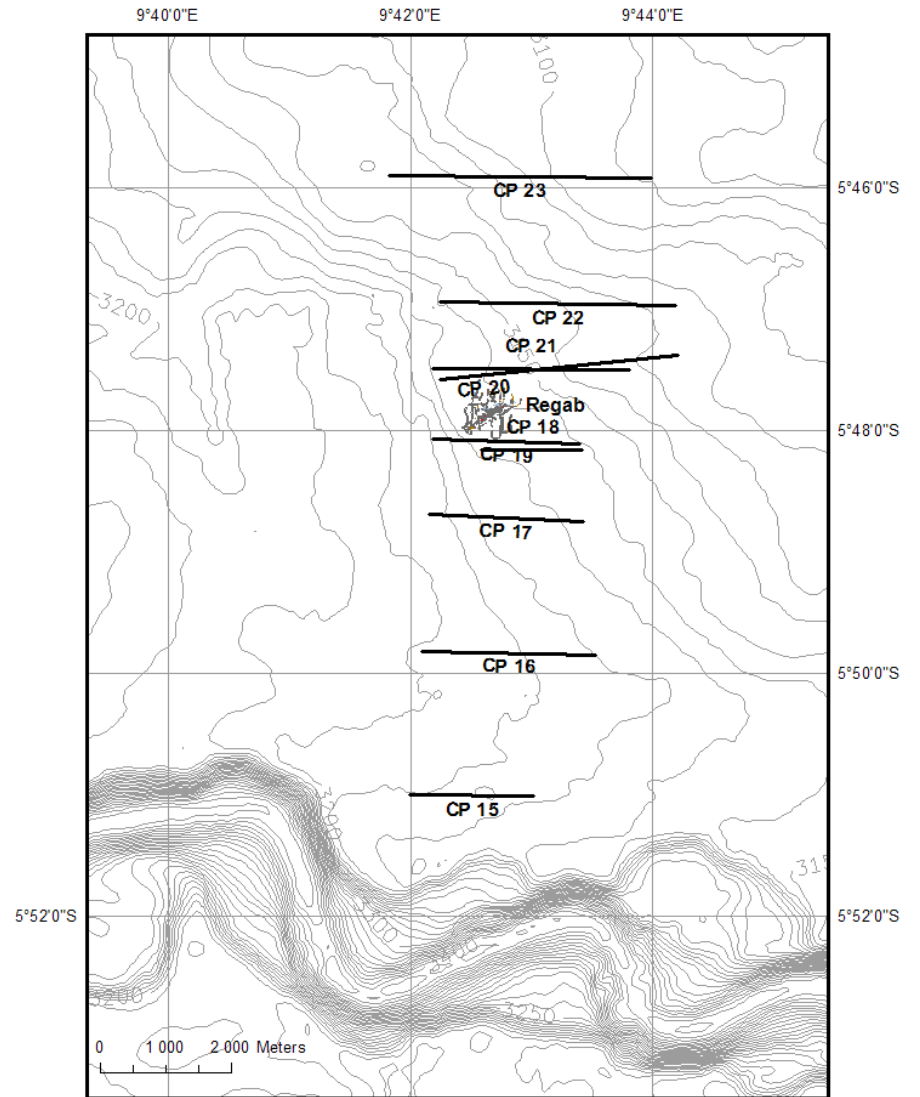
891

892 Figure 6:  $\delta^{13}\text{C}$  vs  $\delta^{15}\text{N}$  values of shrimps *Alvinocaris muricola* (a) and holothurids *Chiridota*  
893 sp. (b) from different sites dominated either by mytilids (M) or vesicomysids (V) with  
894 signature of the bivalves at the different sampling sites and sediment for  
895 holothurids.(c) from left to right: *A. muricola* among mussels, *Chiridota* sp. in mussel  
896 and vesicomysid aggregates.  
897

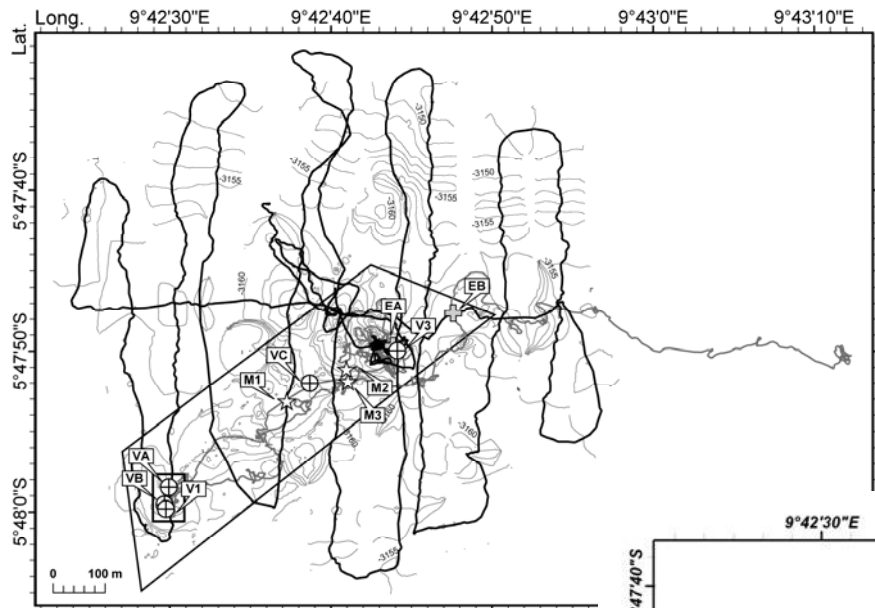


a.

Fig. 1

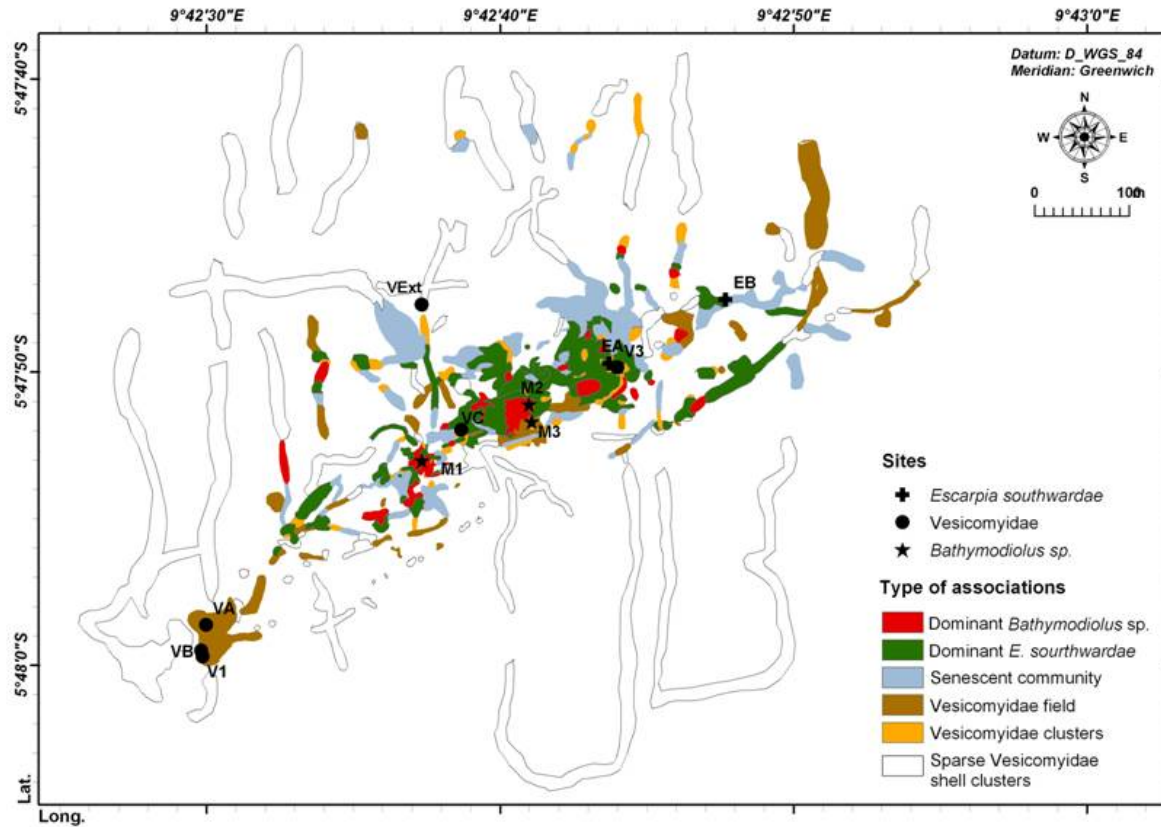


b.

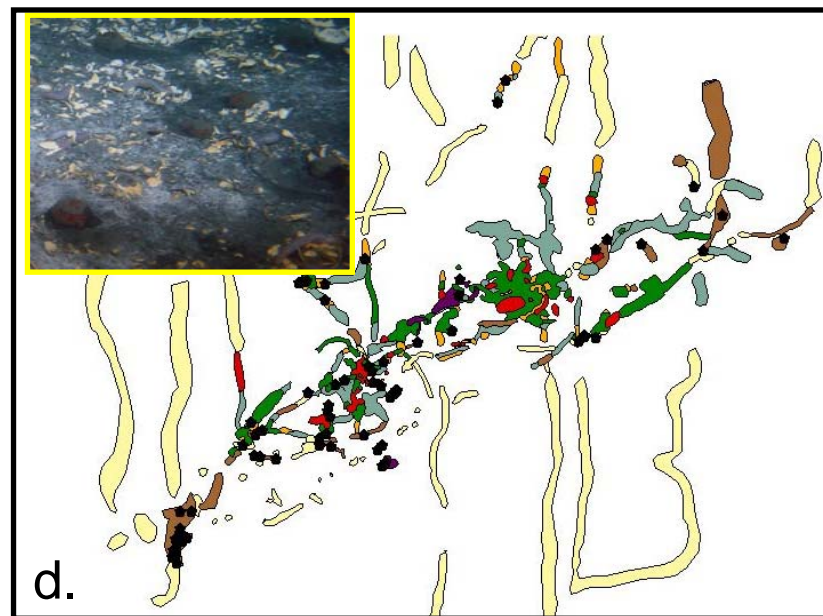
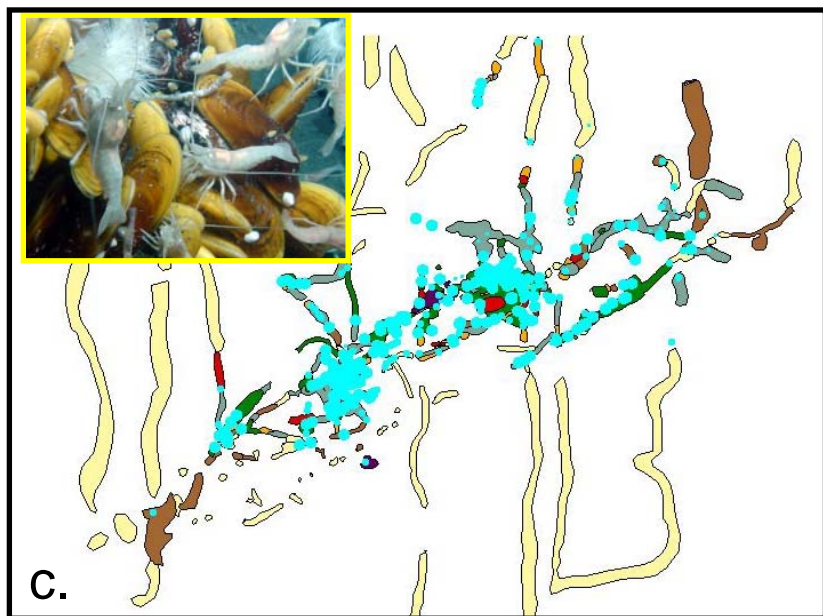
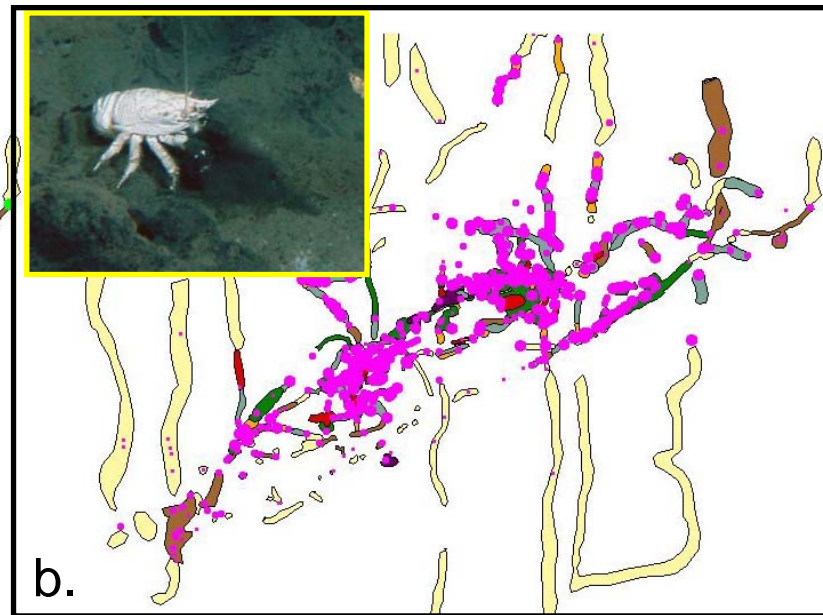
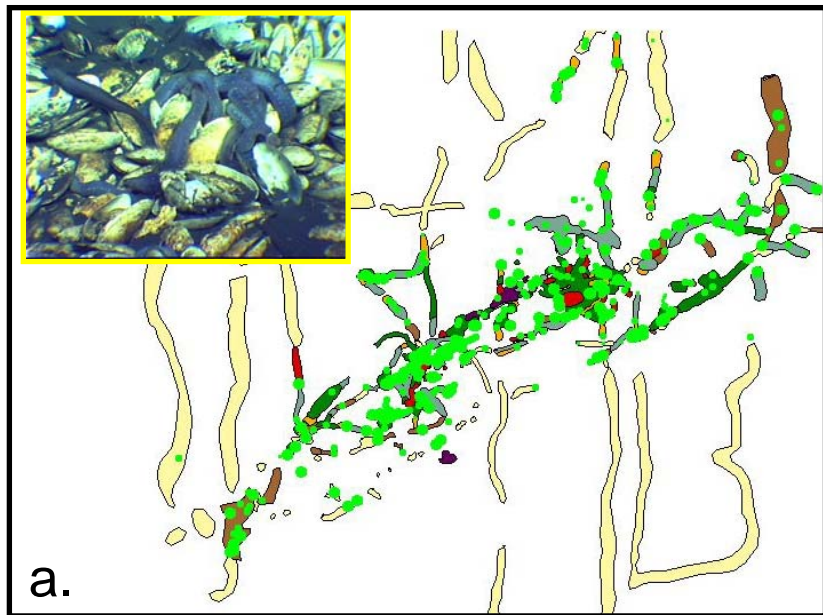


a.

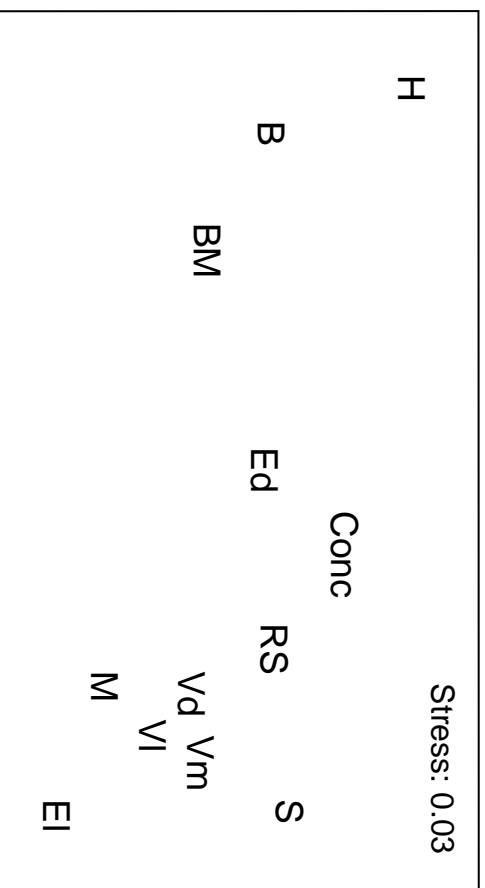
Fig 2



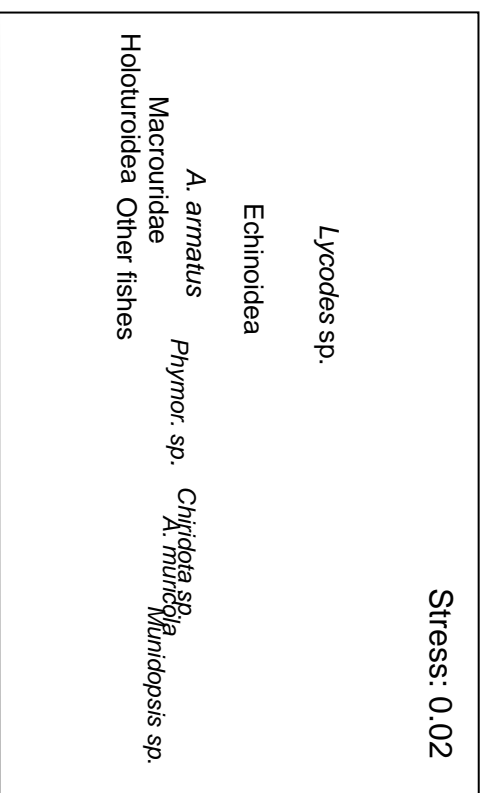
b.

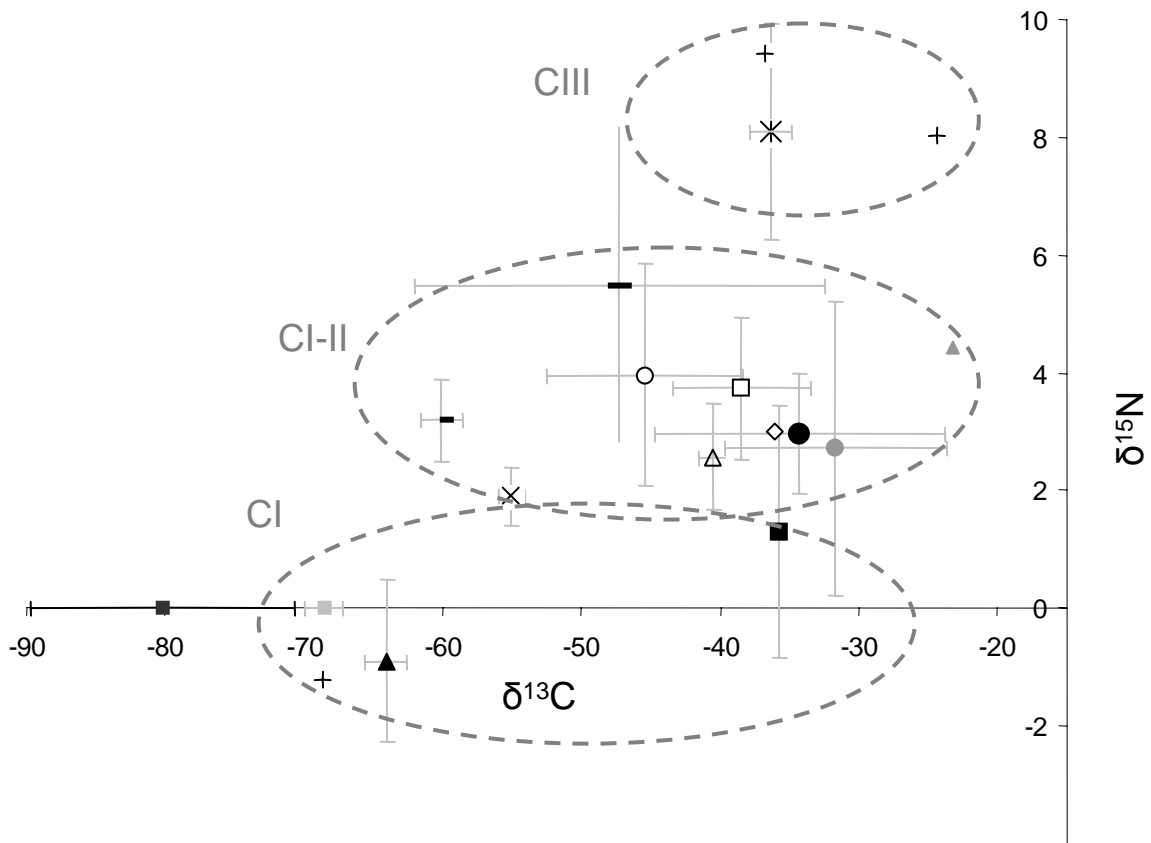


a.

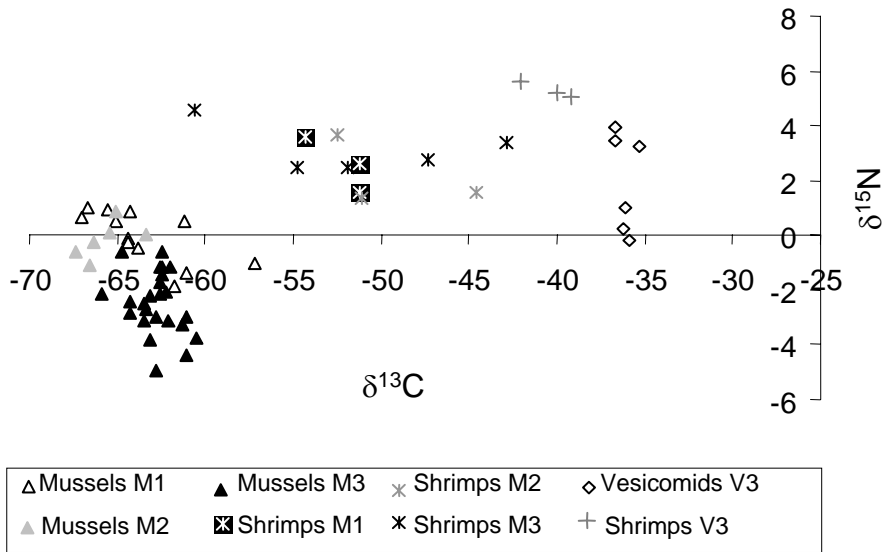


b.

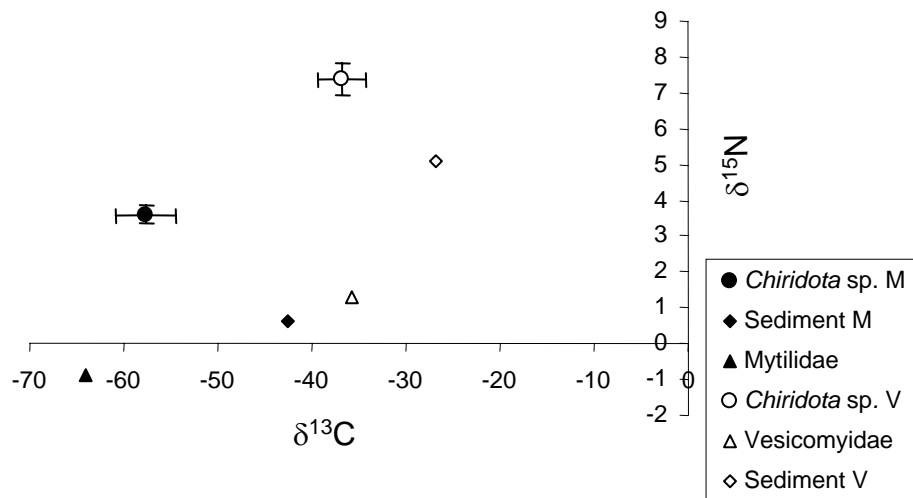




a.



b.



c.



Table 1.

Characteristics of the sampling sites based on dominant symbiont-bearing species.

Site	Dominant species	Percentage of living individuals	Cluster size (m <sup>2</sup> )	Other comments
M1	Mytilidae <i>Bathymodiolus</i> aff. <i>boomerang</i> <sup>a</sup>	100	400	
M2	<i>B. aff. boomerang</i>	100	1	
M3	<i>B. aff. boomerang</i> <sup>a</sup>	100	4	
V1	Vesicomidae: <i>Laubiericoncha chuni</i>	>80	4	External, main large field
VB	Vesicomidae	0	Unknown	External, main large field
Vext	Vesicomidae	c. 50	0.45	External, isolated cluster
V3	Vesicomidae: <i>Calyptogena regab</i>	>80	0.35	Central zone
VC	Vesicomidae	>80	0.75	Central zone
EA	Siboglinidae: <i>Escarpia southwardae</i>	c. 100	<0.5	Adults (>1.5 m long)
EB	<i>E. southwardae</i>	c. 100	<0.25	Young bush (<0.5 m long)

Table 2.

Densities (ind m<sup>-2</sup>) (a) and biomass (g dry weight m<sup>-2</sup>) (b) of megafauna species from image analysis and sampling in the clusters defined by symbiont-bearing species (M: clusters dominated by mytilids; V: by vesicomysids, E: by escarpiids).

	M1	M2	M3	V3	VC	V1	VB	Vext	EA	EB
(a)										
<b>Symbiont-bearing species</b>										
Bivalvia										
<i>B. aff. boomerang</i>	591.7	1066.7	869.4							
Vesicomysidae				741.6	607.5	586.4	0 (sh.)	66.7		
Polychaeta										
<i>E. southwardae</i>	125.0		189.2						769.1	250.0
<b>Associated species</b>										
Actiniaria	52.8	13.5	3.03					4.2		
Gastropoda										
<i>Paralepetopsis</i> sp.	227.8	236.3	68.7						79.5	
<i>Provanna</i> sp.	508.3	87.8	129.3	210.4	38.8	67.8			105.8	

	<b>M1</b>	<b>M2</b>	<b>M3</b>	<b>V3</b>	<b>VC</b>	<b>V1</b>	<b>VB</b>	<b>Vext</b>	<b>EA</b>	<b>EB</b>
<i>Phymorhynchus</i> sp.					3.0	30.3	27.8		2.8	
Crustacea										
<i>Alvinocaris muricola</i>	450.0	344.3	743.7	245.6	53.4	0.7	55.6	0	302.4	58.5
<i>Munidopsis geyeri</i>						8.1	27.8			2.7
Holothuridea										
<i>Chiridota</i> sp.	2.8	6.8		93.3	4.9		111.1			31.9
Chordata										
<i>Lycodes</i> sp.						2.8		2.1		
<b>Total</b>	<b>1958.3</b>	<b>1741.8</b>	<b>2003.2</b>	<b>1290.9</b>	<b>707.5</b>	<b>696.1</b>	<b>222.3</b>	<b>73.0</b>	<b>1256.7</b>	<b>343.1</b>
Associated species	1313.9	675.1	1130.9	549.3	100.0	107.0	222.3	6.3	487.6	93.08
(b)										

	M1	M2	M3	V3	VC	V1	VB	Vext	EA	EB
<b>Symbiont-bearing species</b>										
Bivalvia										
<i>B. aff. boomerang</i>	1966.9	3546.0	2890.2							
Vesicomysidae				1964.5	1609.2	1553.2	0	0		
Polychaeta										
<i>E. southwardae</i>	91.4		138.4						562.2	90.0
<b>Associated species</b>										
Actiniaria	n. e.							n.e.		
Gastropoda										
<i>Paralepetopsis</i> sp.	1.8	1.8	0.53						0.64	
<i>Provanna</i> sp.	10.4	1.8	2.65	4.3	0.8	1.4			2.22	
<i>Phymorhynchus</i> sp.					3.0	29.9	27.5		2.8	
Crustacea										
<i>Alvinocaris muricola</i>	255.0	195.1	421.4	139.2	30.2	0.4	31.5	0	171.3	33.2

	<b>M1</b>	<b>M2</b>	<b>M3</b>	<b>V3</b>	<b>VC</b>	<b>V1</b>	<b>VB</b>	<b>Vext</b>	<b>EA</b>	<b>EB</b>
<i>Munidopsis geyeri</i>						23.0	78.6			7.5
Holothuridea										
<i>Chiridota</i> sp.	3.4	8.3		114.6	6.0		136.4			0.7
Chordata										
<i>Lycodes</i> sp.						n.e.		n.e.		
Total	>2329	3753.1	3453.2	2222.6	1649.1	>1608	222.3	n.e.	736.4	126.4
Associated species	270.6	207.1	401.3	258	39.9	54.8	222.3	n.e.	174.2	36.4

n.e.: non-estimated.

Table 3.

Isotopic carbon signature ( $\delta^{13}\text{C}$ ) of methane extracted from sediment or expelled fluid on the REGAB pockmark.

Sampling site	Sample type	% CH <sub>4</sub>	$\delta^{13}\text{C}$ CH <sub>4</sub> (‰)
Vesicomysid field	Sediment	100	-82
Regab centre	Sediment	99.8	-81
Regab centre	Gas from sediment core	99.8	-84.3
Hydrate outcrop	Gas from sediment core	100	-68.5
Next to M2	Sediment	99.94	-68.7
Next to M1	Sediment	99.87/99.92	-84.8/-96.2
Regab centre	Fluid	99.941	-70.4
Regab centre	Fluid	99.954	-68.69
Regab bubble site	Fluid	99.989	-67.3
Regab bubble site	Fluid	99.955	-67.9

Table 4.

Isotopic signatures of sediment and particles sampled by cores or traps in and off the REGAB pockmark.

Sample	$\delta^{13}\text{C}$ (‰) mean	$\delta^{13}\text{C}$ (‰) sd	$\delta^{15}\text{N}$ (‰) mean	$\delta^{15}\text{N}$ (‰) sd
Sediment M1	-30.9		0.14	

Sample	$\delta^{13}\text{C}$ (‰) mean	$\delta^{13}\text{C}$ (‰) sd	$\delta^{15}\text{N}$ (‰) mean	$\delta^{15}\text{N}$ (‰) sd
Sediment M2	-47.69	2.37	1.36	0.34
Sediment M3	-29.46		0.07	
Sediment V1	-25.58		5.72	
Sediment V2	-26.4		3.92	
Sediment V3	-28.04	0.72	4.44	0.37
Particulars from traps	-23.22		4.43	
Sediment 600 m/1700 m from Regab	-23.77	0.59	7.88	0.03

Table 5.

Isotopic signatures of symbiont-bearing species from different sampling sites in the REGAB pockmark.

Species/sites	$\delta^{13}\text{C}$ (‰) mantle	$\delta^{13}\text{C}$ (‰) gill	$\delta^{15}\text{N}$ (‰) mantle	$\delta^{15}\text{N}$ (‰) gill	$\delta^{13}\text{C}$ (‰) mean*	$\delta^{15}\text{N}$ (‰) mean*
<i>Bathymodiolus</i> aff. <i>boomerang</i>						
M1	-63.3±3.5 (12)	-63.7±2.1	-0.5±0.8 (12)	-0.6±0.3		
M2	-64.5±0.8 (6)	-67.0±0.8	0.3±0.5 (6)	-0.7±0.4		
M3	-63.7±1.5 (24)	-62.4±0.9	-1.9±0.9 (24)	-3.1±1.0		
<i>Vesicomidae</i> sp.						

Species/sites	$\delta^{13}\text{C}$ (‰) mantle	$\delta^{13}\text{C}$ (‰) gill	$\delta^{15}\text{N}$ (‰) mantle	$\delta^{15}\text{N}$ (‰) gill	$\delta^{13}\text{C}$ (‰) mean*	$\delta^{15}\text{N}$ (‰) mean*
V1	-35.6±1.6 (5)	-35.7±1.1	2.9±2.0 (5)	-1.0±2.1		
V3	-36.0±0.8 (5)	-36.0±0.15	3.5±0.3 (5)	2.9±2.0		
<i>Escarpia southwardae</i>						
M1					-24.2±5.5 (5)	2.5±1.6 (5)
EA (adults)					-36.22±3.3 (5)	2.9±0.6 (5)
EB (youngs)					-29.1±3.4 (3)	–

Table 6.

Mean isotopic signatures of associated megafauna sampled by ROV in the clusters dominated either by mytilids (M), vesicomysids (V) or escarpids (E) or by trawl (CP20) in the REGAB cold-seep site.

Species	Site	$\delta^{13}\text{C}$ (‰) mean	$\delta^{13}\text{C}$ (‰) sd (n)	$\delta^{15}\text{N}$ (‰) mean	$\delta^{15}\text{N}$ (‰) sd (n)
Polychaeta					
<i>Branchipolynoe</i> sp.	M1	-60.09	–	2.46	–
Gastropoda					
<i>Provanna</i> sp.	VB,E2E3	-35.12	1.66 (6)	3.89	1.33 (6)
	CP20	-44.31	4.43 (5)	4.71	0.49 (5)

Species	Site	$\delta^{13}\text{C}$ (‰) mean	$\delta^{13}\text{C}$ (‰) sd (n)	$\delta^{15}\text{N}$ (‰) mean	$\delta^{15}\text{N}$ (‰) sd (n)
<i>Paralepetopsis</i> sp.	M1	-55.0	–	1.9	–
<i>Phymorrhynchus</i> sp.	E2	-36.13	1.46 (3)	No value	–
	CP20	-36.03	1.51 (5)	2.99	0.41 (5)
Crustacea					
<i>Alvinocaris muricola</i>	M1M2M3	-50.4	0.92 (11)	2.6	0.45 (11)
	V3	-40.4	1.47 (3)	5.3	0.26 (3)
	CP20	-38.5	2.03(3)	4.40	0.54 (3)
<i>Munidosis geyeri</i>	E2	-36.31	–	9.37	–
	CP20	-36.33	1.05 (3)	6.50	0.42 (3)
<i>Munidopsis hirtella</i>	CP20	-22.4	–	11.25	–
Echinodermata					
<i>Chiridota</i> sp.	M1M3	-57.06	5.59 (5)	3.93	1.96 (5)
	CP20	-36.78	1.84 (2)	7.37	0.49 (2)
Echinidae sp.	Near to M3	-41.29	2.53 (3)	1.95	1.25 (3)

Species	Site	$\delta^{13}\text{C}$ (‰) mean	$\delta^{13}\text{C}$ (‰) sd (n)	$\delta^{15}\text{N}$ (‰) mean	$\delta^{15}\text{N}$ (‰) sd (n)
Chordata					
<i>Lycodes</i> sp.	CP20	-43.23	22.83 (3)	5.41	5.79 (3)

Table 7.

Isotopic signature ( $\delta^{13}\text{C}$ ) of fishes sampled by trawls at increasing distance from the REGAB site and estimated percentages of chemosynthetic material in their diet.

Trawls	$\delta^{13}\text{C}$ (‰) mean (n)							Mean	% chemosynthetic material
	CP17	CP18	CP19	CP20	CP21	CP22	CP23		
<b>Distance from REGAB</b>	<b>1560 m</b>	<b>580 m</b>	<b>400 m</b>	<b>610 m</b>	<b>680 m</b>	<b>1660 m</b>	<b>3600 m</b>		
<i>Acantaurus armatus</i>	-20.1 (2)		-21.8 (3)	-22.7	-19.3	-22.4 (2)	-22.0	-21.4±1.6	4–27
<i>Bassossetus robustus</i>	-20.6 (2)				-25.0	-21.2 (4)	-23.2 (2)	-21.7±1.6	16–39
<i>Coryphaenoides striaturus</i>	-18.8						-18.8	-18.8±0.6	7
<i>Porogadus milles</i>	-21.5 (2)	-22.0		-18.6		-21.0		-21.0±1.5	6–23
<i>Malacoteus niger</i>		-18.7						-18.7±1.0	6

	$\delta^{13}\text{C}$ (‰) mean ( <i>n</i> )							Mean	% chemosynthetic material
	CP17	CP18	CP19	CP20	CP21	CP22	CP23		
<b>Trawls</b>									
<b>Distance from REGAB</b>	<b>1560 m</b>	<b>580 m</b>	<b>400 m</b>	<b>610 m</b>	<b>680 m</b>	<b>1660 m</b>	<b>3600 m</b>		
<i>Scopeloberyx robustus</i>		-18.5			-21.2			-19.9±1.6	19
<i>Holcomystronus squamosus</i>			-21.3	-28.3				-24.8±3.8	20–56
<i>Stomias boa boa</i>			-18.1 (2)			-15.9		-17.5±1.7	0–3
<i>Stylephorus chordatus</i>			-20.7		-22.6			-21.8±1.1	17–26
<i>Histobranchius bathybius</i>						-18.0		-18.0±0.1	0
<i>Manducus maderensis</i>				-21.1		-16.9		-19.0±2.6	6
<i>Lycodes</i> sp.				-45.2 (3)				-45.2±19.7	35–100
<i>Munidopsis geyeri</i>			-34.4 (2)	-36.3 (3)					86–100
<i>Munidopsis hirtella</i>			-23.6 (2)	-22.0		-21.4			19–31